DEPOSITION OF Cu-BTC ON PULP AND TEXTILE FIBERS FOR SENSOR APPLICATION

A Thesis Submitted to
the Graduate School of Engineering and Sciences of
İzmir Institute of Technology
in Partial Fulfillments of the Requirements for the Degree of

MASTER OF SCIENCE

in Chemical Engineering

by
Cemal GÜNER

December 2018
İZMİR

We approve the thesis of **Cemal GÜNER**

Examining Committee Members:

Prof. Dr. Fehime ÇAKICIOĞLU ÖZKAN
Department of Chemical Engineering, İzmir Institute of Technology

Prof. Dr. Günseli ÖZDEMİR
Departement of Chemical Engineering, Ege University

Assist. Prof. Dr. Erdal UZUNLAR
Departement of Chemical Engineering, İzmir Institute of Technology

28 December 2018

Prof. Dr. Fehime ÇAKICIOĞLU ÖZKAN
Supervisor, Department of Chemical Engineering
İzmir Institute of Technology

Prof. Dr. Erol ŞEKER
Head of the Department of Chemical Engineering

Prof. Dr. Aysun SOFUOĞLU
Dean of the Graduate School of Engineering and Sciences

ACKNOWLEDGMENT

I offer my deepest appreciation and gratitude to my advisor, Prof. Dr. Fehime ÇAKICIOĞLU ÖZKAN for her supervision, support, encouragement and patience in all steps of my study. I would like to thank Viking Kağıt ve Selüloz A.Ş. for their support. I would also like to thank the technical staff who carried out the FT-IR, ATR-IR, XRD, SEM, NH_3 adsoprtion analysis.

I would like to thank my parents, Tuncay HEPDURLUK and Tülay GÜNER, and my grandmother, Perihan GÜNER, because they always supported and encouraged me.

I would like to thank my dear friends, Ceren ORAK, Merve DİKMEN, Canan TAŞ, Özenç AKOVA, Muhammet EREN for their endless support, encouragement, patience and helps.

I would like to thank my wife, Emine SOLMAZ GÜNER, for her patience, endless support and love.

ABSTRACT

DEPOSITION OF Cu-BTC ON PULP AND TEXTILE FIBERS FOR SENSOR APPLICATION

Cu-BTC is synthesized from Copper(II) nitrate and benzene-1,3,5-tricarboxylic acid and it is one of the most common metal organic framework which is used for catalysis, sensing, controlled release, separation and storage processes. The application areas of Cu-BTC could be increased by deposition on different surfaces. Cu-BTC is positively charged and to deposit Cu-BTC on a surface, the surface must have negative charge. The most common natural material with negative charge is cellulose. Raw pulp fibers, cotton and viscose fabrics are rich in terms of cellulose, so they were used as cellulose source.

The aim in this study is to deposit Cu-BTC on pulp fibers, cotton and viscose fabrics and then, to investigate their sensing properties. In order to investigate whether Cu-BTC was deposited on cotton, pulp, and viscous fibers or not, a characterization study was carried out to investigate their properties. In this context, XRD, SEM, FT-IR, ATR-IR analysis were performed. As a result of the characterization study, it was concluded that the Cu-BTC was deposited on the pulp, cotton fibers, and viscous successfully. The Cu-BTC deposited substrates showed sensing activity against humidity and NH_3 gas.

ÖZET

SENSÖR UYGULAMASI İÇİN Cu-BTC'NİN KAĞIT VE TEKSTİL LİFLERİNDE BİRİKTİRİLMESİ

Cu-BTC, Bakır (II) nitrat ve Benzen-1,3,5-trikarboksilik asitten sentezlenir ve kataliz, duyarlılık (belirli gazlara karşı), kontrollü salınım, ayırma ve depolama işlemleri için kullanılan en yaygın metal organik yapılardan biridir. Cu-BTC'nin uygulama alanları farklı yüzeylere tutturulmasıyla arttırılabilir. Cu-BTC pozitif yüklüdür ve bir yüzeyde Cu-BTC'nin tutunabilmesi için yüzeyin negatif yüklü olması gerekir. Negatif yüklü en yaygın doğal malzeme selülozdur. Ham kağıt hamuru lifleri, pamuk ve viskon kumaşlar selüloz açısından zengindir, bu nedenle selüloz kaynağı olarak kullanılmıştır.

Bu çalışmada, Cu-BTC'nin pamuk, kağıt hamuru ve vorteks lifleri üzerine tutturulması amaçlanmış ve daha sonra asensör özellikleri araştırılmıştır. Cu-BTC'nin kağıt lifleri, pamuk ve viskon kumaşlar üzerinde tutunup tutunmadığını araştırmak ve özelliklerini araştırmak için bir karakterizasyon çalışması yapılmıştır. Bu kapsamda XRD, SEM, FT-IR, ATR-IR analizleri yapıldı. Karakterizasyon çalışması sonucunda, Cu-BTC'nin kağıt hamuru, pamuk ve viskon kumaşlar üzerinde başarılı bir şekilde tutunduğu sonucuna varılabilir. Cu-BTC tutunan bu malzemeler nem ve NH_3 gazına karşı duyarlılık göstermiştir.

TABLE OF CONTENTS

Page

LIST OF FIGURES

Figure **Page**

LIST OF TABLES

Table **Page**

CHAPTER 1

INTRODUCTION

Metal-organic frameworks (MOFs) which are prepared in the form of one, two or three-dimensional networks using inorganic salts and multidentate organic linkers have recently gained considerable attention due to their large surface areas, large internal pore volume and ability to bear various functionalities. Due to these reasons, MOFs have a wide range of application areas such as gas storage, adsorption/separation, and catalysis. They could be prepared in some various forms such as beads, pellets and thus, a low-pressure drop and high performance could be obtained in the industrial applications. The complete usage of the inner surface of MOFs could be obtained by the deposition of MOFs on suitable substrates rather than the encapsulation of them decreases if encapsulated (Siegle and Kaskel, 2009; Abdelhameed et al., 2017).

MOFs are deposited on several different surfaces in literature. Cui et al. (2009) studied MOF films on stainless steel fibers for the solid-phase microextraction of volatile and harmful benzene homologs (Cui et al., 2009). Yehia et al. (2004) synthesized matrix membranes by mixing poly(3-acetoxyethylthiophene) and MOFs and the synthesized MOFs provided selectively methane adsorption (Yehia et al., 2004). Keskin and Sholl (2010) also reported that the addition of particles to a polymeric matrix represents an important method for enhancing the performance of these polymeric materials for potential applications in gas separation processes (Keskin and Sholl, 2010). Kaskel et al. (2011) studied the immobilization of Cu-BTC (MOF-199) in polymers (polystyrene, polyvinylpyrrolidone, and polyacrylonitrile) by electrospinning to obtain composite fibers with MOF particles (Kaskel et al., 2011).

MOFs can be deposited on the several surfaces by various methods which are mainly solvothermal method, colloidal deposition, layer-by-layer (LBL) liquid phase epitaxy, and microwave-assisted thermal deposition. Among these methods, LBL is an important method to obtain MOF deposited surfaces which are used for selective separations and sensors (Nijem et al., 2015). Different types of MOFs such as Ln-MOF, ZIF-8 can be used in sensor applications. One of the most widely studied MOF is Cu-

BTC (copper benzene tricarboxylate), also known as MOF 199 or HKUST-1. For instance, Pinto et al. (2012) synthesized Cu-BTC and the synthesized Cu-BTC was attached on the surface of cellulosic fibers chemically. Cu-BTC has open metal sites so that it can provide high storage capacities for gases like hydrogen and methane (Pinto et al., 2012). Thus, Cu-BTC could be used as a gas sensor. Besides, MOF199 consists of dimeric cupric tetracarboxylate units with a short Cu–Cu internuclear separation since it has a blue color, so the deposition of it on to the cellulosic substrates can be verified by optically (Pinto et al., 2012).

The aim of this study is to synthesize Cu-BTC and its deposition on different materials such as pulp fiber, cotton fabric, and viscose fabric for sensing activities. These materials consist of cellulose which is an abundant material in nature. Among these materials, cotton fabric has less carboxylic groups than the others. In order to increase the carboxylic groups of cotton fabric carboxymethylation process is carried out. Consequently, carboxymethylated cotton fabric, pulp fiber and viscose fabric have abundant carboxylic groups to deposite Cu-BTC on their surfaces. Additionally, pulp fibers have very high flexibility and could be easily molded into sheets by various inexpensive methods. Because of these reasons, these materials were chosen to test the sensing activity of Cu-BTC. The characterization study of Cu-BTC deposited materials is carried out by XRD, SEM, FT-IR and ATR-IR analysis to investigate the crystalline structure, surface morphology and framework vibration of all samples, respectively.

CHAPTER 2

METAL ORGANIC FRAMEWORKS (MOFs)

Metal-organic frameworks (MOFs), which are also called as porous coordination polymers (PCP), are compounds of metal ions or clusters coordinated to organic ligands to form one, two or three-dimensional structures. The structure and properties of MOFs depend on the choice of metal and binder molecule (organic molecules) (Batten et al., 2013).

MOFs are highly porous compounds with vast internal surface areas (Tranchemontagne, D. et al., 2009). The diversity of metal ions, organic linkers, and pore geometry provide nearly an infinite number of combinations. The usage areas of MOFs have been recently increased since they have well-defined pore sizes, extremely high permanent porosity, significant thermal stability and the ability to design pore geometry and chemical functionality (Luebbers, M. Et al., 2010).

MOFs can be used for catalysis, adsorption, gas separation, gas purification, gas storage, drug delivery, and sensing activity. MOFs have a porous structure with tunable sizes and also their chemical structures can be adjusted so that they are suitable for gas separation and gas storage, particularly hydrogen, methane and carbon dioxide. Hydrogen is one of the most important substances. Hydrogen is a clean energy source and an important reactant in various chemical processes in industry. The storage of hydrogen is the biggest difficulty. In order to overcome that difficulty, MOFs provide a solution. MOFs can generally store hydrogen by van der Waals interactions but using metal nodes which can adsorb hydrogen via metallic bonding to these porous structures increases storage capacity and effectiveness greatly (Yamauchi et al., 2009). In order to obtain the maximum performance from MOFs by increasing their physisorption forces, the structure, pore chemistry and pore sizes of MOFs are adjusted. Besides, the addition of metal and metal oxide particles to MOFs showed great potential for the separation of noble gases (Rowsell and Yaghi, 2005).

Almost 90 % of the processes in the chemical industry is carried out in the presence of the catalysts which are generally metals. However, the metal catalysts need

support materials to become more active and stronger catalysts for some chemical processes. So, the choice of suitable support material has a great importance (Astruc et al., 2005). Nanoparticles are generally used as catalysts due to their high surface area-to-volume. However, using nanoparticles as catalysts has some drawbacks which are a tendency to aggregate, low recyclability and the difficulty of recovering the particles from the reaction media. In order to overcome these drawbacks, the supporting materials should be porous with certain pore characteristics to improve the selectivity of the reaction and they should be easily removed from the reaction media. In that respect, MOFs are one of the best support materials because of their tailorable pore size, adjustable surface structure. MOFs can be used as catalyst supports in some reactions; for instance, oxidation of hydrocarbons and alcohols, oxidation of CO, hydrogenation of olefins, hydrogen generation and carbon-carbon coupling. For example, MOF-5 was used as a supporting material and Au was deposited on it. The Au deposited MOF-5 was used as a CO_2 gas sensor (Falcaro et al., 2016).

MOFs can also be used for sensing in plenty of applications such as; medical diagnostics, food/drink quality control, pollutants detection etc. because these applications need sensors to detect specific elements or molecules with high selectivity. If the target molecules interact with certain MOFs, then their photophysical, electrical or mechanical properties change (Xiao et al., 2011). Tailoring the pore size and chemistry MOFs can be made to have this kind of selectivity to be used as sensors. Using them as host for other sensors such as metal nanoparticles have created great potential in sensor applications. Among these applications, the most promising ones are; size-selective sensors, gas-selective sensors, ion-selective sensors and photonic crystal sensors (Falcaro et al., 2016).

Molecular delivery is another important usage area of MOFs. The focus of the controlled release is to optimize attractive forces between the framework and the loaded molecule. The biggest challenge in the controlled release is the spontaneous release of the guest molecules from MOFs. To overcome this problem focusing on the molecular diffusion which is the driving force of the delivery system. To adjust the concentration of guest molecules in the pores and the external environment have great importance in this process as molecular diffusion is all about equilibrium. (Horcajada et al., 2005; Cunha et al., 2013).

2.1. Copper Benzene Tricarboxylate Cu-BTC (MOF 199 or HKUST-1)

In this study, Cu-BTC (copper benzene tricarboxylate), also called as MOF 199 or HKUST-1, was chosen to study sensing activity. Cu-BTC consists of copper nodes, including 1,3,5-benzenetricarboxylic acid struts and its density is about 1.2 g/cm^3. Cu-BTC is mostly used for gas storage, sensor, and separation applications. The adsorption behavior of Cu-BTC was investigated for CO_2, H_2 and sulfur compounds. The structure of Cu-BTC is shown in Figure 2. 1.

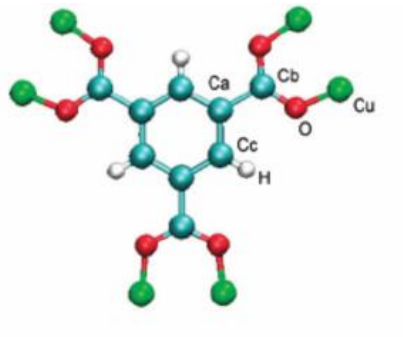

Figure 2. 1. Structure of Cu-BTC

Cu-BTC can be synthesized by the conventional synthesis which is carried out by conventional electric heating without any parallelization of reactions. One of the main parameters is reaction temperature for conventional synthesis. Depending on the reaction temperature, conventional synthesis can be divided into two main groups which are solvothermal and nonsolvothermal reactions. While non-solvothermal reactions can occur below or at the boiling point and under ambient pressure, solvothermal reactions may take place at room or elevated temperatures.

The compositional parameters such as molar ratios of starting materials, pH, type of solvent, and the process parameters such as reaction time, temperature, and pressure are varied for the synthesis of Cu-BTC. In order to investigate the effect of these parameters on the size, shape, and structure of Cu-BTC, the high-throughput (HT) methods for solvothermal syntheses has been recently developed (Stock et al., 2012).

Ex situ and in situ methods are used to investigate the crystallization mechanism and to optimize the synthesis conditions. The crystal size of the final product can be adjusted by these methods. While in situ studies require the use of special equipment and

synchrotron radiation, ex-situ studies do not need any special equipment and can easily be conducted in laboratory (Stock et al., 2012).

In addition to these methods, alternative synthesis methods which are microwave-assisted, electrochemical, mechanochemical, and sonochemical have recently been developed. Microwave-assisted synthesis depends on the interaction of electromagnetic waves with mobile electric charges which could be polar solvent molecules/ions in a solution or electrons/ions in a solid. When the appropriate frequency is applied, the collision between the molecules will occur, which cause an increase in kinetic energy. It is an energy efficient method of heating because of the direct interaction of the radiation with the solution/reactants. The electrochemical method is a facile and environmentally friendly approach to control the reactant concentration over a period of time. In addition, by controlling the anodic oxidation, different rates of metal ions can be added to the solution. In mechanochemical method, the mechanical breakage of intramolecular bonds is followed by a chemical transformation. In sonochemical method, a chemical change takes place in the reaction mixture depending on the application of high-energy ultrasound irradiation from 20 kHz to 10 MHz. The homogenous nucleation centers occur by the ultrasound irradiation, so that Cu-BTC crystallization time can decrease (Pirzadeh et al., 2017; Stock et al., 2012).

2.1.1. Application of Cu-BTC

Cu-BTC can be used for catalysis, adsorption, gas separation, gas purification, gas storage, drug delivery, biomedical and sensor applications (Neufeld et al., 2015; Čejka, J., 2012). In literature, there are many studies about the applications of Cu-BTC and some of them will be summarized in this section and the sensor applications will be explained in the next section.

Cu-BTC can be used as a catalyst for the CO oxidation and Cu-BTC show complete conversion of CO at 140 °C (Yang et al., 2018). Additionally, Cu-BTC can be used as an adsorbent to capture CO_2. For instance, Nobar synthesized Cu-BTC at a modest reaction temperature and duration by applying pre-mixing to the precursor solutions. The most stable Cu-BTC was obtained when the precursors were highly diluted and it showed stable CO_2 adsorption capacity. In another study, Cu-BTC was used as an adsorbent for

the hydrogen purification and the effect of adsorption pressure and flow rate on the breakthrough process, and adsorption pressure, feeding time and feeding rate in four-step PSA cycles for hydrogen purification performance are investigated. According to the parametric study results, when higher adsorption pressure (7 bar), shorter feeding time (192 s) and lower feeding flow rate ($2.46x10^{-4}$ mol/s) were used, higher hydrogen purity could be obtained. However, lower recovery and productivity was observed at these conditions. In literature, there are many studies about the Cu-BTC for the controlled release of drugs. For instance, 5- fluorouracil (FU, which is a drug) was incorporated in Cu-BTC and its slow delivery from the Cu-BTC was investigated. The optimum proportion of 5-FU and Cu-BTC was found as 0.82 g:1.0 g and a slow release profile was observed when the 82 % of the drug was released from Cu-BTC in 48 hours (Lucena et al., 2013).

2.2. Chemical Sensing

The detection of toxic chemicals is a significant issue to protect people to prevent the inhalation of toxic chemicals. If the toxic chemicals were not detected, then many people could be affected from the toxic chemicals. MOFs have chemical sensing properties and they could be used to detect several hazardous gases such as ammonia, chlorine, cyanogen chloride, hydrogen sulfide, nitrogen dioxide, nitrogen oxide, sulfur dioxide, phosphine, arsine, radon. Volatile organic compounds (VOCs) could also be detected by MOFs. For example, cyclohexane, benzene, toluene, p-xylene, o-xylene, m-xylene, ethylbenzene, halogenated and noncyclic hydrocarbons could be detected by MOFs (Woellner et al., 2018).

Cu-BTC has ability to interact with chemicals so that it has chemical sensing property. In literature, there are many studies about the chemical sensing property of Cu-BTC. Cu-BTC is used for detecting the presence of hazardous chemicals such as ammonia, arsine, and hydrogen sulfide gases. Cu-BTC is used to detect the hydride gases which are ammonia, arsine, and hydrogen sulfide (Peterson et al., 2015). Hazardous gases which are sulfur dioxide, chlorine, radon, cyclohexane, tetrahydrothiophene, benzene, toluene, dichloromethane, and ethylene oxide are also detected by Cu-BTC (Woellner et al., 2018).

In this study, Cu-BTC deposited on different type of textiles such as pulp fiber, cotton fabric, and viscose fabric will be used for the detection of ammonia gas by the help of chemical sensing property of Cu-BTC.

2.3. Deposition of Cu-BTC

The deposition of Cu-BTC on different substrates provides an easy way to use for sensor activity in various fields. The deposition of Cu-BTC on different substrates could be obtained by solvothermal and non-solvothermal processes. The most important process parameter is the reaction temperature for these processes. While non-solvothermal reactions can occur below boiling point and under ambient pressure, solvothermal reactions may take place at room or elevated temperatures (Zhuang et al. 2015).

Synthesis of Cu-BTC is generally done solvothermally in a mixed solvent system which is also followed in this study. $Cu(NO_3)_2.3H_2O$ is dissolved in deionized water and mixed with trimesic acid (H_3BTC: benzene-1,3,5-tricarboxylic acid) which is dissolved in ethanol. And then, the solution is heated to a certain temperature above the boiling point of the mixture. The synthesis reaction is represented by the equation below (Pinto et al., 2012):

$$2Cu(NO_3)_2.3H_2O + 2H_3BTC \rightarrow \underbrace{[Cu_3(BTC)_2].3H_2O}_{\boldsymbol{Cu-BTC}} + 6HNO_3 \qquad (2.1)$$

The deposition of Cu-BTC on different substrates was summarized in Table 1. Before the deposition process, sometimes the surface of the support material should be charged with required ions to increase the effectiveness of the deposition process. For deposition of the Cu-BTC, carboxymethylation is used to obtain a suitable charge on the surface of cellulose substrates. Cu-BTC is deposited on the pulp fibers surface to be used in filtration industry. Pulp fibers were flexible and could easily be molded into sheets. Three different pulp fibers, which are CTMP, a bleached southern pine kraft pulp and unbleached kraft pulp were used as substrates in the deposition of Cu-BTC. According to the results, Cu-BTC was easily deposited on the pulp fibers which had higher lignin content (Küsgens et al., 2009).

Zhuang et al. deposited Cu-BTC onto plastic, paper, and textile substrates by inkjet printing of a precursor solution containing dimethylsulfoxide (DMSO), ethanol and ethylene glycol. Cu-BTC contained solvent was used as ink and desired patterns were easily printed via inkjet printers. Cu-BTC does not have a certain shape and is not oriented and densely grown crystals were observed on the surface of printed substrates. While hierarchical pore structure and high density of Cu-BTC were observed on the foil surface, low density of Cu-BTC was observed on the office paper due to its complex morphology. Cu-BTC containing ink was printed on the textile substrates to capture hazardous gases such as NH_3, HCl, and H_2S vapor. The printed substrates were exposed to these gases and a color change was observed in each of them. The turquoise color of the substrates was turned to dark blue, yellow, and brown rapidly after exposure to NH_3, HCl, and H_2S vapor, respectively. Consequently, Cu-BTC containing ink printed textile substrates could be used as label-free, inexpensive, and practical gas sensors (Zhuang et al., 2013).

The deposition of Cu-BTC on the cotton fabric surface is done in order to be used as NO generation catalyst. Cu-BTC deposited cotton fabric was used as a catalyst for NO generation from a substrate (S-nitrosocyseamine) and the reaction rate was observed as 19.0 ± 3.0 nMs^{-1}(Neufeld et al., 2015).

Abbasi et al. deposited Cu-BTC on silk fibers under ultrasound irradiation to provide antibacterial activity. The effect of pH, reaction time, ultrasound irradiation, and sequential dipping steps on the deposition of Cu-BTC on silk fibers were investigated. FT-IR results show that the bond formation between $–COO^-$ and Cu^{2+} was observed so that the deposition was performed successfully. Cu-BTC on the silk fibers was crystalline and its amount increased due to the increasing number of dipping steps. The Cu-BTC deposited silk fibers showed high antibacterial activity against *Escherichia coli* and *Staphylococcus aureus*. They (Abbasi et al., 2012).

Pinto et al. deposited Cu-BTC on cotton, a cellulosic fibrous, substrate and then tested for gas selectivity and toxic chemicals removal. In order to investigate the importance of carboxylate groups onto the surface of anionic cellulose. According to the results, the attachment of Cu-BTC on the cotton surface was obtained successfully and the order of addition of $Cu(OAc)_2$-copper acetate, BTH3, 1,3,5-benzenetricarboxylic acid, and TEA-triethylamine was found as critical factors for chemical attachment and growth of Cu-BTC on cotton. XPS analysis was carried out to determine the copper density on the cotton surface and the higher density of copper on the cotton surface was

observed when the A and C procedures were used to chemical attachment of Cu-BTC. Additionally, the presence of Cu-BTC on the cotton surface was confirmed via FT-IR analysis. The characteristic lengths of Cu-BTC crystals were determined by SEM analysis and they were between 200 nm to a few microns (Pinto et al., 2012).

Meilikhov et al. deposited Cu-BTC on polymers in the form of porous material so that they have a wide range of textile applications such as gas separation materials and protection layers for working clothes. In order to increase the amount of Cu-BTC on the polymer surface, the amino groups at the polyester surface are reacted with a bromoacetic acid to enhance the reactive groups on the surface. The step-by-step deposition method could be used as a reproducible way for multiple deposition cycles and the surface morphology and perfectness could easily be controlled by this method.

Viscose fabrics have numerous binding sites so that they provide good affinity for polar compounds. The high cost of adsorbents led to search new alternative materials like MOFs. Abdelhameed et al., (2017) studied Cu-BTC deposited viscose fabric for fuel purification to improve the quality of petroleum-derived products.

As seen above, use of Cu-BTC deposited substrates such as printing ink, pulp, cotton, and viscose fabric have not been yet demonstrated for detection of NH_3 gas in the literature. So, an experimental study was carried out to investigate the sensing activity of Cu-BTC deposited on those substrates.

Table 2. 1. Deposition processes of Cu-BTC and the application areas of Cu-BTC deposited substrates

Substrate	Pre-treatment of Substrates	Metal Source	Deposition Process	Synthesis Temperature	Application Area	References
Cotton Fabric	-	Copper Nitrate	-Inkjet Print	85°C	-Gas Seperation	Zhuang et al. (2013)
	Carboxymethylation process	Copper Acetate	-Layer by Layer	Room Temperature	-Biomedical material	Neufeld et al. (2015)
	Carboxymethylation process	Copper Acetate	-Stirring with Copper and BTC solutions respectively	Room Temperature	-Gas Seperation	Silva Pinto et al. (2012)
	Carboxymethylation process	Copper Nitrate	-Layer by Layer	Room Temperature	-Antibacterial material	Rubin et al. (2018)
Pulp Fiber	-	Copper Nitrate	-Stirring with Cu-BTC Solution	85°C	-Filter	Küsgen et al. (2009)
Polyester Fabric	PVA modification	Copper Acetate	-Stirring with Copper and BTC solutions respectively	Room Temperature	-Pyrazine Adsorption	Meilikhov et al. (2011)
Silk Fabric	Alkaline pH	Copper Acetate	-Stirring with Copper and BTC solutions respectively	Room Temperature	-Antibacterial Material	Abbasi et al. (2011)
Viscose Fabric	-	Copper Nitrate	-Stirring with Cu-BTC Solution	Room Temperature	-Fuel Purification	Abdelhameed et al. (2017)

CHAPTER 3

EXPERIMENTAL STUDY

3.1. Materials

Pulp fibers and cotton fabric were purchased from Viking Kağıt ve Selüloz A.Ş and Gamateks, respectively. Copper (II) nitrate trihydrate, benzene-1,3,5-tricarboxylic acid (trimesic acid), ethanol, N-dimethylformamide (DMF), sodium hydroxide and sodium chloroacetate were obtained from Emsure and Sigma Aldrich.

3.2. Cu-BTC Synthesis and Deposition on Pulp Fibers

1.68 g (8 mmol) of trimesic acid was dissolved in 100 ml Ethanol:DMF (1:1 v/v) solution and were mixed with a 50 ml aqueous solution of 1.86 g (8mmol) $Cu(NO_3)_2.2.5\ H_2O$. 1 g of short fibers was added to the solution and was stirred for about 15 min. The mixture was heated to 85 °C in a 400 ml vessel and kept at this temperature for 24 h. At the same time, in order to investigate the stirring effect, the mixture was stirred at 85 °C for 24 h. After 24 h, the stirred and non-stirred products were separately filtered and washed with Ethanol:H_2O mixture to get rid of impurities. After that, the stirred and non-stirred short pulp fibers (SF) were dried at room temperature for a short amount of time. Lastly, in order to activate these fibers, they were put in an oven at 160 °C for 18 h. The activation of short fibers was also obtained at 85 °C to investigate the temperature effect. The same procedure was repeated for and long pulp fibers (LF). The experimental procedure is illustrated in Scheme 1 and also, some pictures of experimental steps are given in Figure 3. 1.

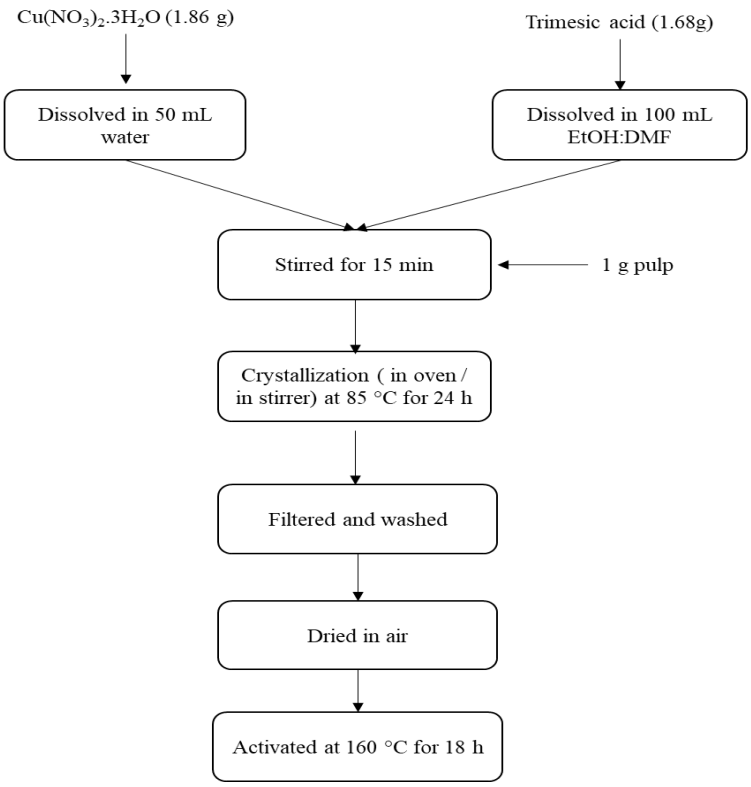

Scheme 1. Steps of the Cu-BTC deposition on pulp fibers (Küsgen et al., 2013).

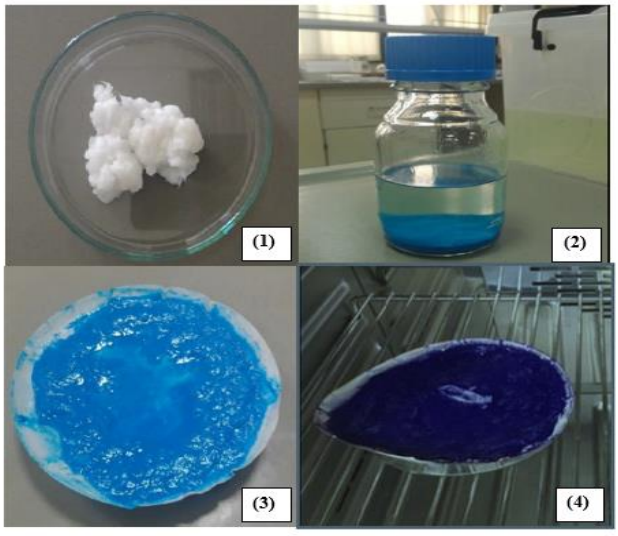

Figure 3. 1. Raw pulps (1), pulp fibers in solution after 24h stirring (2), after the filtering and washing process (3) and after the activation (4).

Due to the adsorption of the water molecules on the Cu-BTC, a color difference between the third and fourth images was observed. The color of Cu-BTC after the activation process was dark. As the adsorbed water amount increased on the Cu-BTC surface, the color of Cu-BTC became lighter blue. Additionally, to understand the effect

of stirring, the same process was followed without using a stirrer and in that process, the mixture was put into the oven for 24 h.

3.3. Cu-BTC Synthesis and Deposition on Cotton Fabric

In order to deposite Cu-BTC on cotton fabric, firstly, the cotton fabric should be carboxymethylated to obtain anchoring points. Then, Cu-BTC was deposited on the cotton fabric. The detail of these two steps is given below.

3.3.1. Carboxymethylation of Cotton Fabric

The cotton fabric must be carboxymethylated with sodium chloroacetate in the presence of sodium hydroxide to obtain more carboxyl groups to deposite Cu-BTC onto the cotton fabric. Hence, an anchoring point was obtained by the carboxymethylation for the deposition of Cu-BTC onto the cotton fabric. The reaction mechanism of carboxymethylation of cotton and the deposition mechanism of Cu-BTC on cotton fabric are given in Figure 3. 2.

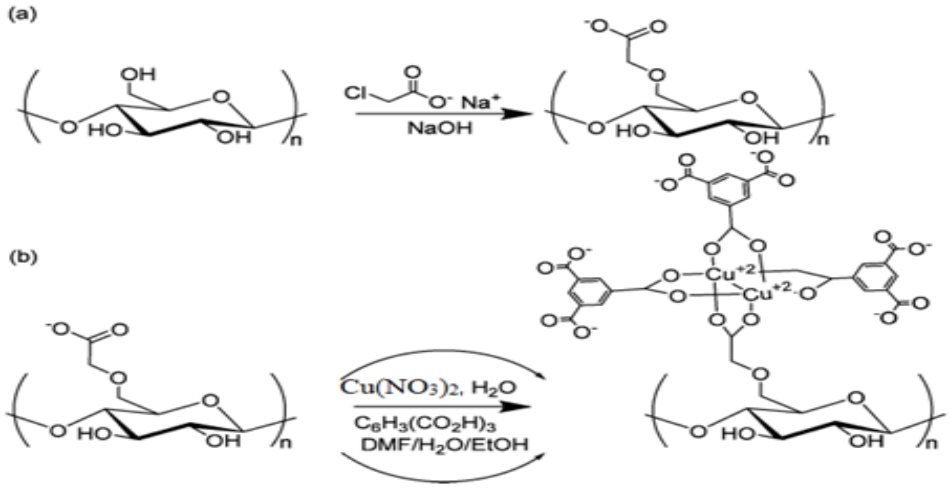

Figure 3. 2. Carboxymethylation of cotton fabric (a), deposition process on cotton fabric(b).

Two different carboxymethylation procedures were used to prepare the cotton fabrics for the deposition of Cu-BTC. The first carboxymethylation process was carried out using 100 ml 15 wt% NaOH solution (2:1 ethanol deionized water). The cotton fabric was added into the solution and stirred for 30 min. Then, the cotton fabric was removed and 11.6 g sodium chloroacetate was added into the solution. After that, the cotton fabric was put into the solution again and stirred for 1 h. The cotton fabric was removed from the solution and immersed into deionized water for 30 min. Then, it was washed with deionized water and ethanol, respectively. The cotton fabric was firstly dried at the room temperature and then it was dried in the oven for 1 h at 60 °C. The first carboxymethylation procedure was given in Scheme 2.

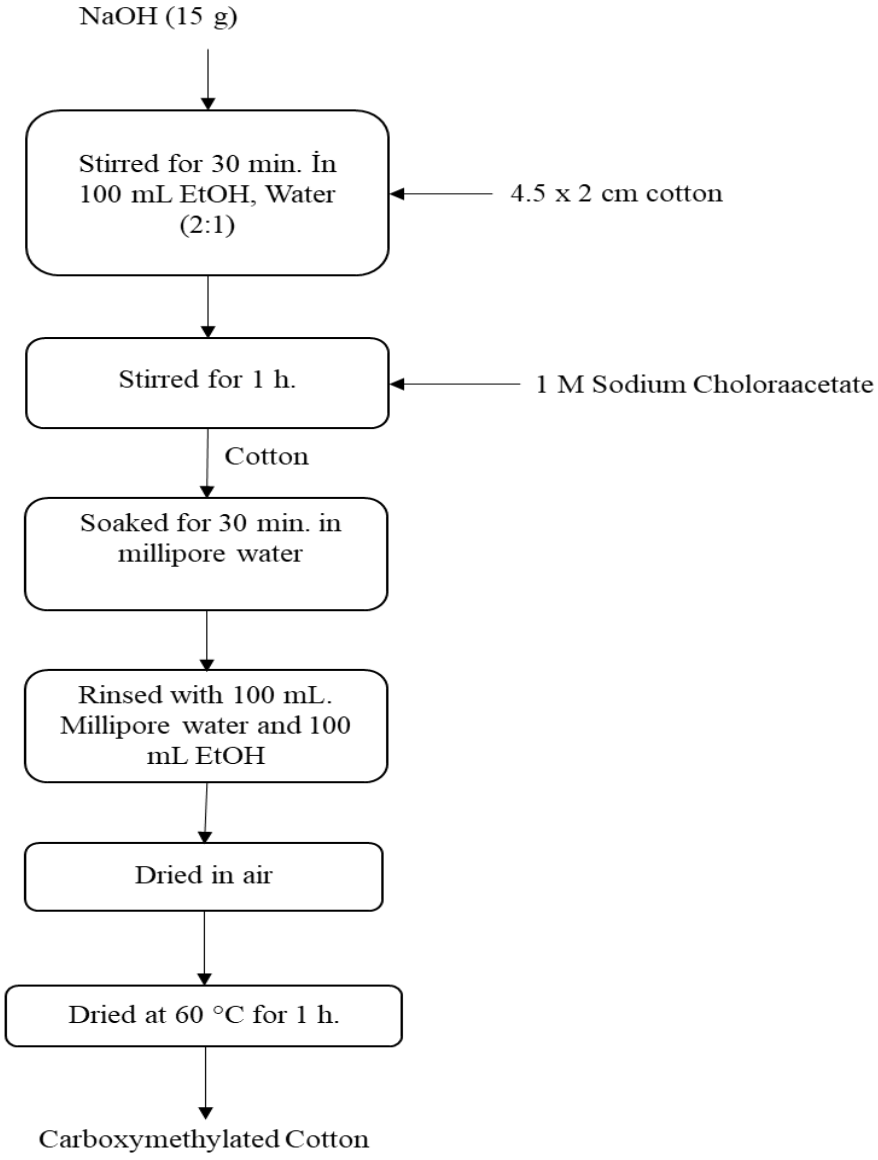

Scheme 2. Carboxymethylation procedure of cotton (Rubin et al., 2018).

To obtain an anchoring point for the deposition of Cu-BTC onto the cotton fabric, another carboxymethylation procedure was applied. In this procedure, cotton fabric was carboxymethylated with sodium chloroacetate in the presence of sodium hydroxide. A 1 M solution of sodium chloroacetate was prepared in 15 wt % sodium hydroxide, and the cotton fabric was immersed into the solution and stirred for 1 h. The second carboxymethylation procedure is given in Scheme 3.

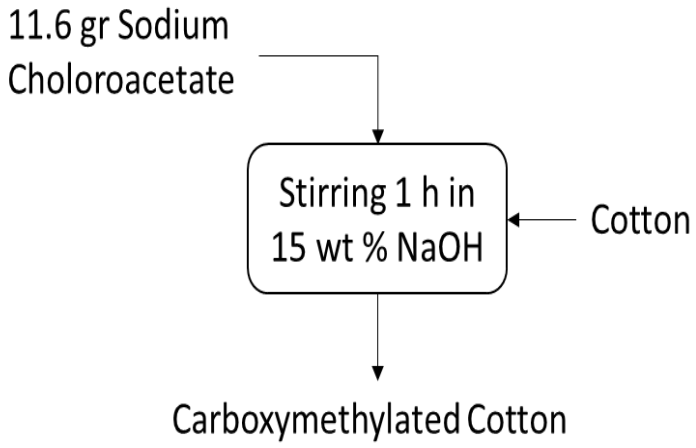

Scheme 3. The second carboxymethylation procedure of cotton (Neufeld et al., 2015).

3.3.2. Deposition of Cu-BTC

After carboxymethylation step, 860 mg $Cu(NO_3)_2.2.5H_2O$ was mixed in a 12 ml of DMF:ethanol:water (1:1:1) mixture and a piece of cotton fabric were put into the mixture. After stirring them for overnight 500 mg trimesic acid was dissolved in DMF:ethanol:water (1:1:1) mixture and added to the mixture dropwise and kept stirring for 24 h. After stirring the cotton fabric, the obtained Cu-BTC deposited cotton fabric was separately washed with distilled water, DMF and ethanol for 5 h to get rid of non-attached Cu-BTC crystals. Lastly, the Cu-BTC deposited cotton fabric was dried in air. The first deposition procedure is given in Scheme 4. The raw cotton fabric and the Cu-BTC deposited cotton fabric are given in Figure 3. 3.

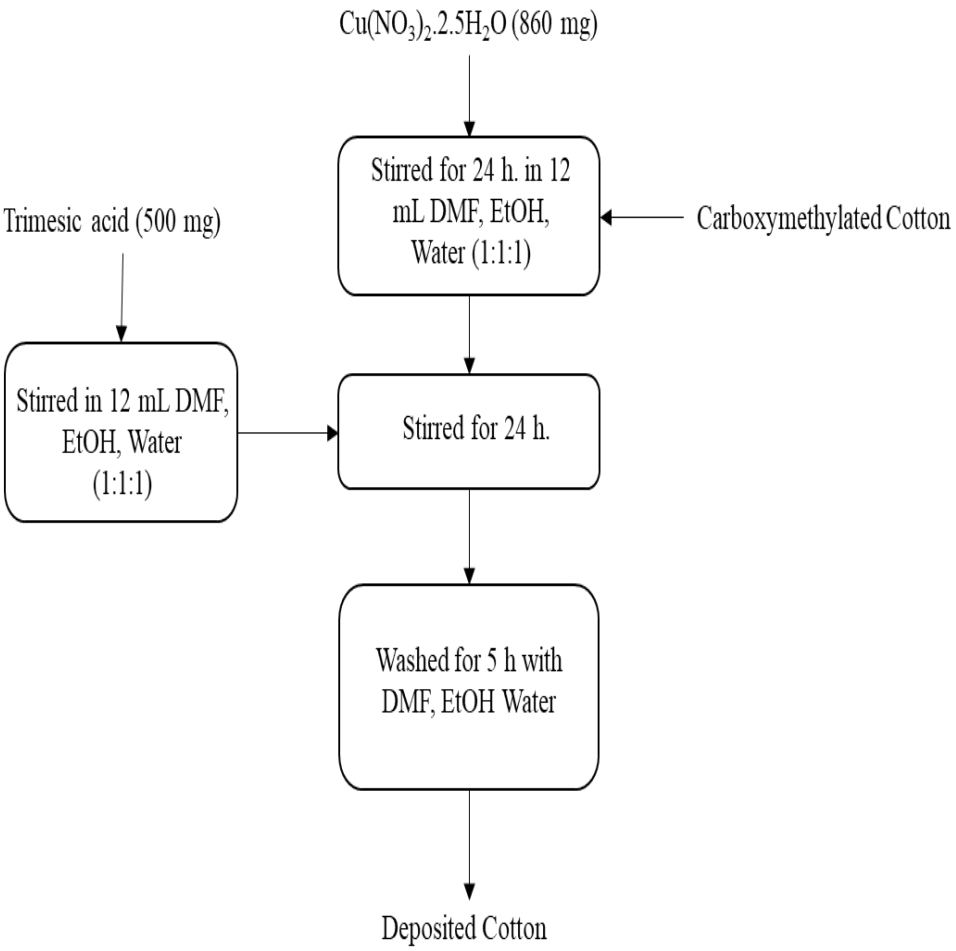

Scheme 4. The steps of first deposition method (Pinto et al., 2012).

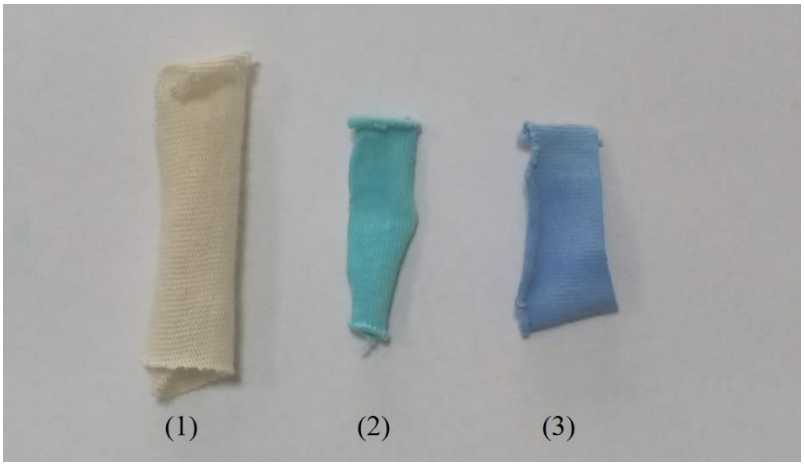

Figure 3. 3. The raw cotton fabric (1), and Cu-BTC deposited cotton fabric (2), Cu-BTC deposited cotton fabric exposed to NH3 gas (3).

Cu-BTC deposition on the cotton fabric was also carried out by layer-by-layer growth. Firstly, copper containing solution was prepared using 1.9 g copper nitrate and 1:1:1 DMA, ethanol and deionized water. Secondly, ligand-containing solution was prepared using 675 mg of trimesic acid and 2:1:1 DMA, ethanol and deionized water. The cotton fabric was first immersed into the copper containing the solution for 17 min and then it was immersed into the ethanol solution for 5 s. The cotton fabric was immersed into the ligand containing solution for 17 min and then it was immersed into the ethanol solution for 5 sn. This cycle was repeated for 15 times. After that, the cotton fabric was soaked into the ethanol for overnight. Finally, the cotton fabric was washed with ethanol solution for six times to remove undeposited Cu-BTC particles. The second deposition procedure is given in Scheme 5.

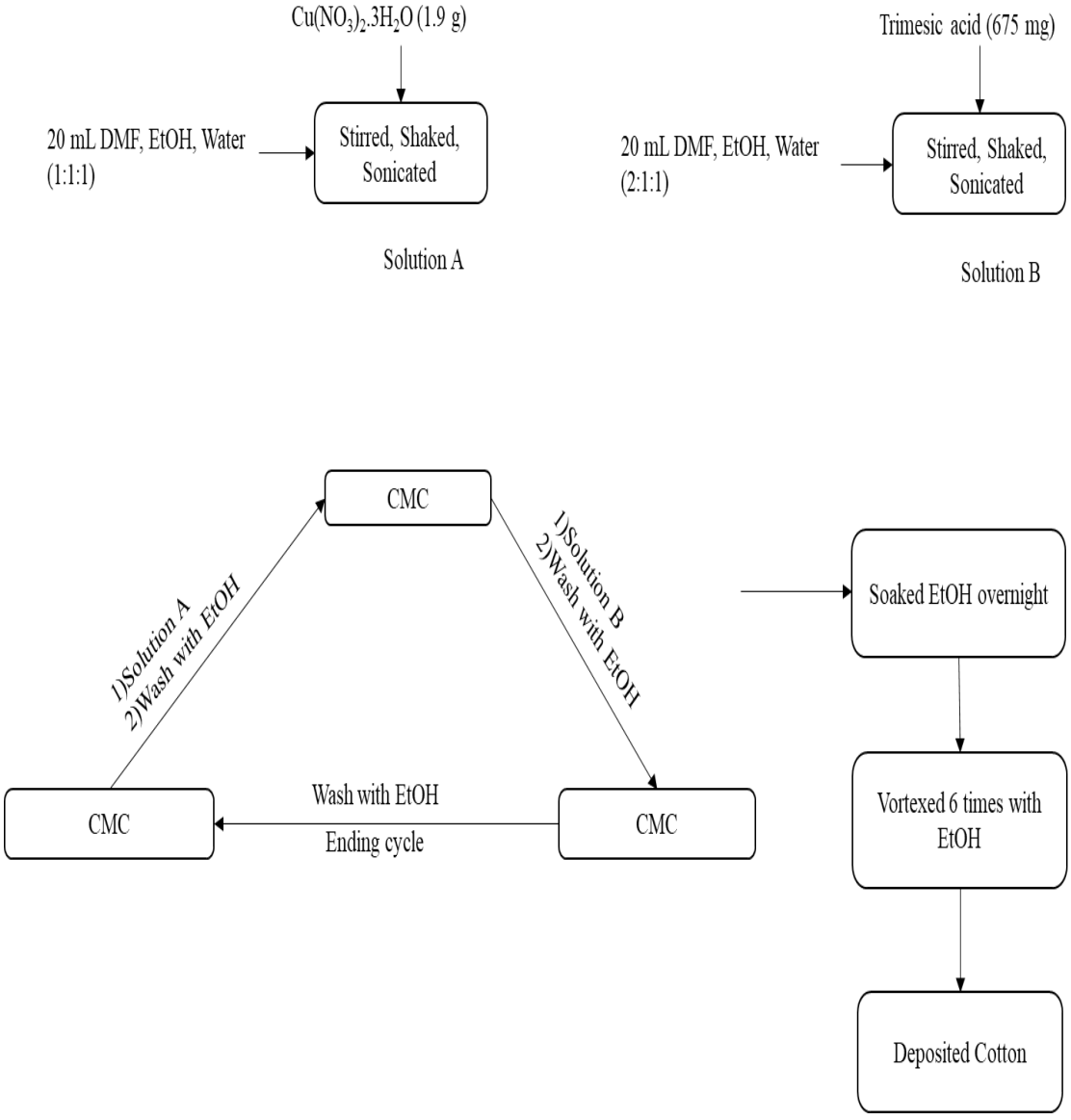

Scheme 5. The steps of the second deposition method (Rubin et al., 2018).

Cu-BTC deposition on the cotton fabric was also carried out by layer-by-layer growth. Firstly, 1.078 g copper acetate was dissolved in 15 mL Millipore water to obtain solution A. Then, to obtain solution B, 631 mg of trimesic acid was dissolved in 15 mL of 1:1:1 DMA, ethanol and Millipore water. The cotton fabric was firstly immersed into the solution A for 5 min and then it was rinsed with water. The cotton fabric was immersed in the solution B for 5 min and then it was rinsed with water. This cycle was repeated for 5 times. After that, the cotton fabric was washed with ethanol to remove undeposited Cu-BTC particles. Finally, the cotton fabric was put into the ethanol solution and sonicated. The third deposition procedure is given in Scheme 6.

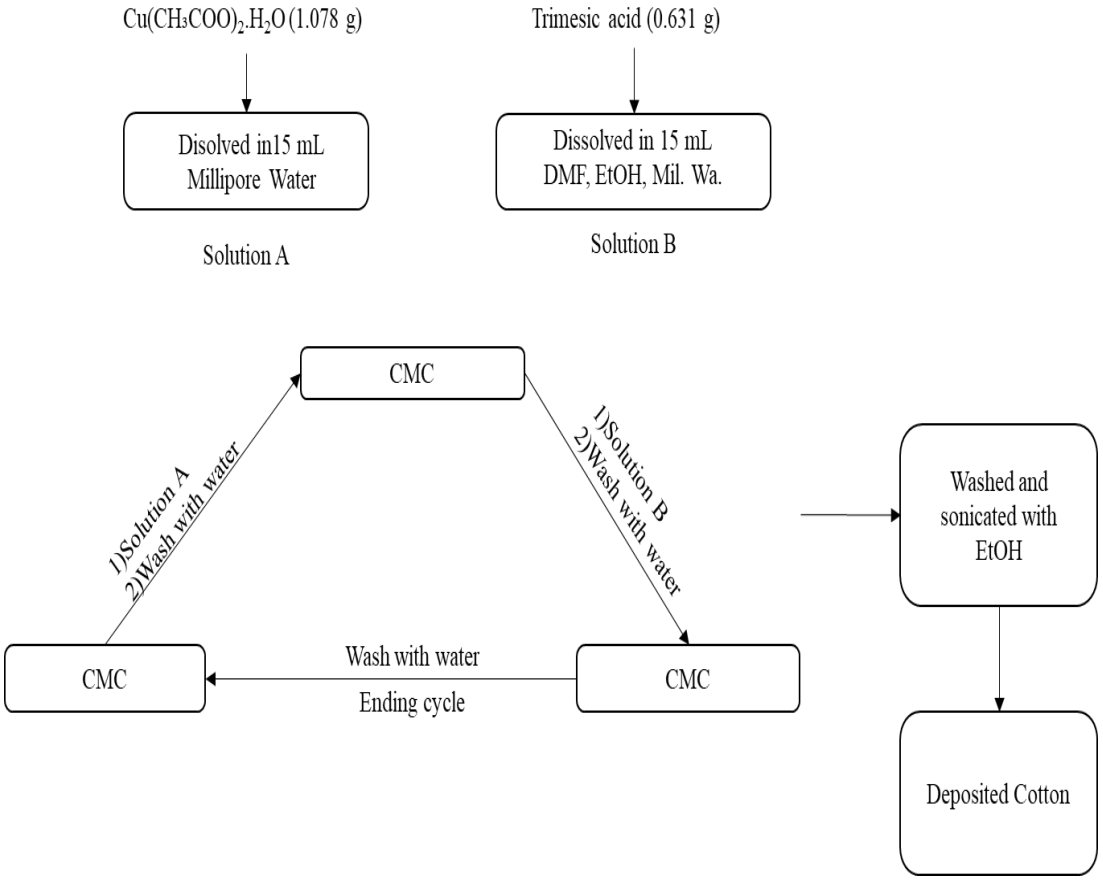

Scheme 6. The steps of the third deposition method (Neufeld et al., 2015).

3.4. Cu-BTC Synthesis and Deposition on Viscose

Firstly, 2.077 g of copper (II) nitrate trihydrate and 1.0 g of trimesic acid were dissolved in 50 mL of DMF because they are highly soluble in DMF. Then, 8×8 cm^2 viscose specimen was added to the solution and stirred for 30 min. The solution mixture

was heated until the complete evaporation of DMF. After that, it was cooled down to room temperature and the Cu-BTC deposited viscose was rinsed with deionized water five times to remove the non-adsorbed and unreacted chemicals. The Cu-BTC deposited viscose was dried in an oven at 75 °C overnight. The procedure of Cu-BTC deposited viscose is given in Scheme 7.

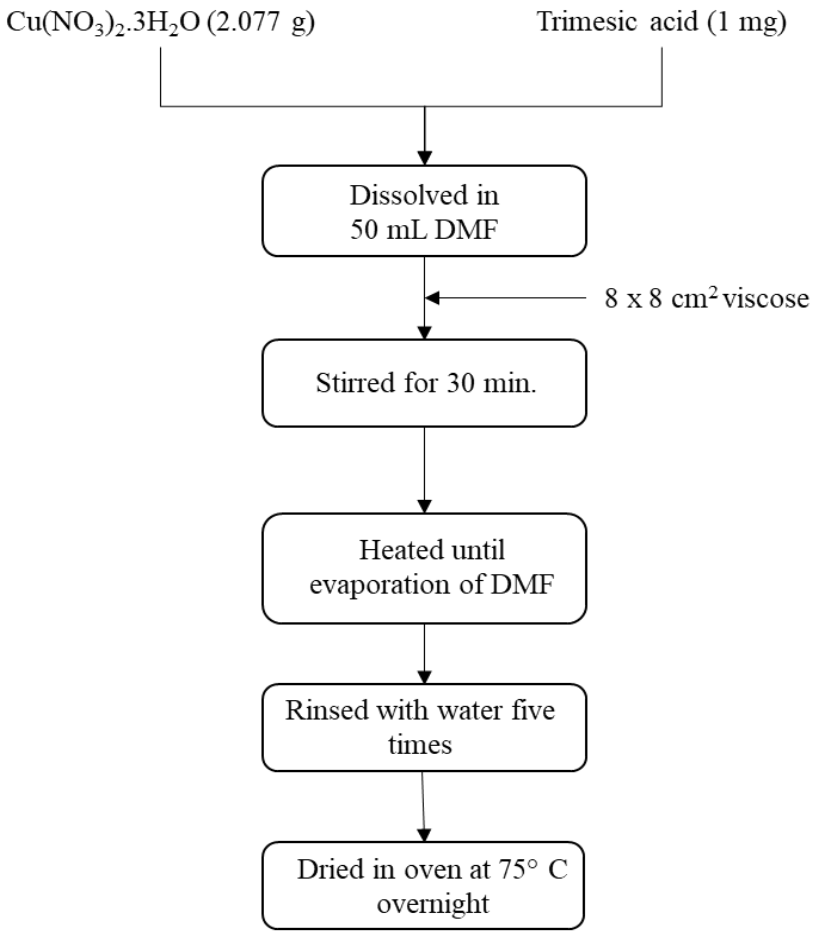

Scheme 7. The procedure of Cu-BTC deposited viscose (Abdelhameed et al., 2017).

3.5. Characterization Studies

The surface morphology of Cu-BTC deposited textiles which are pulp fibers, cotton fabric, and viscose fabric was analyzed via SEM analysis. FEI QUANTA 250 FEG model SEM device was used to analyze the samples.

The framework vibration of synthesized all samples was examined by FT-IR spectroscopy. KBr pellet technique was employed to obtain infrared spectra of the

samples at room temperature. The Cu-BTC deposited cotton fabric and pulp fiber were cut into small pieces and the pellets were prepared with a small pieces amount of 3 wt%. The spectra were retrieved in the wavenumber range of 400–4000 cm^{-1} with a resolution of 4 cm^{-1} by an infrared spectrometer type Shimadzu FTIR 8400S.

The framework vibration of synthesized all samples was also examined by AT-IR analysis. The ATR-IR analysis was performed in the wavenumber range of 650–4000 cm^{-1} via Pelkin Elmer – UATR Two.

The crystalline structures of all samples were determined by X-Ray diffraction type Philips X'Pert diffractometer with CuK radiation. The scattering angle 2Θ was changed from 5° to 63° with a step length of 0.002°.

A gas mixture was used for adsorption of NH_3 onto all samples. The gas to be adsorbed (NH_3) is mixed with a suitable carrier gas, usually helium at a known flow rate. In this study, 50 mL/min He gas was passed through the line for 30 min to clean the line. After that, 40 mL/min of % 10 NH_3 and % 90 He gas mixture was passed through the line for 30 min to comprehend the chemical sensing of Cu-BTC deposited on textiles which are pulp fiber, cotton fabric, and viscose fabric.

CHAPTER 4

RESULTS AND DISCUSSION

The Cu-BTC deposited on pulp fibers, cotton fabric and viscose fabric support were charecterize and sensing properties to NH3 gas was analyzed.

4.1. Characterization Study of Raw and Cu-BTC Deposited Pulp Fibers

As seen from SEM micrograph of synthesized Cu-BTC (Figure 4. 1), the MOF particles have a uniform cubic shape. Same procedure given in Schema 1 was used to deposite Cu-BTC on long and short pulp for period of 6, 12 and 24 h. The effect of strirring was also tested. The SEM micrographs of raw and the stirred Cu-BTC deposited pulp fibers for period of 24 h are represented in Figure 4. 2 in order to observe the crystal growth of Cu-BTC on the pulp fibers. The SEM micrographs of stirred and non-stirred Cu-BTC deposited short and long pulp fibers are given in Figure 4. 3 and Figure 4. 4. for 12 h and 6 h deposition time, respectivelly.

It is obviously seen that the surface of pulp fibers are densely coated with Cu-BTC crystals for each deposition times. The size of the deposited Cu-BTC by non-stirring was bigger than the size of deposited Cu-BTC by stirring. The Cu-BTC crystals have a well-defined shape along the short pulp fibers and the Cu-BTC crystals are regularly distributed along the short pulp fibers for deposition by non-stirring for 12 h. Similar features were observed in another study, which is carried out by Küsgens et al. (Küsgens et al., 2009).

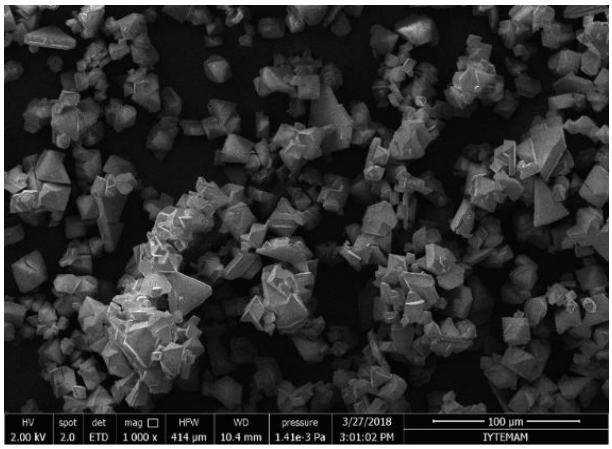

Figure 4. 1. Scanning electron micrograph (SEM) of Cu-BTC.

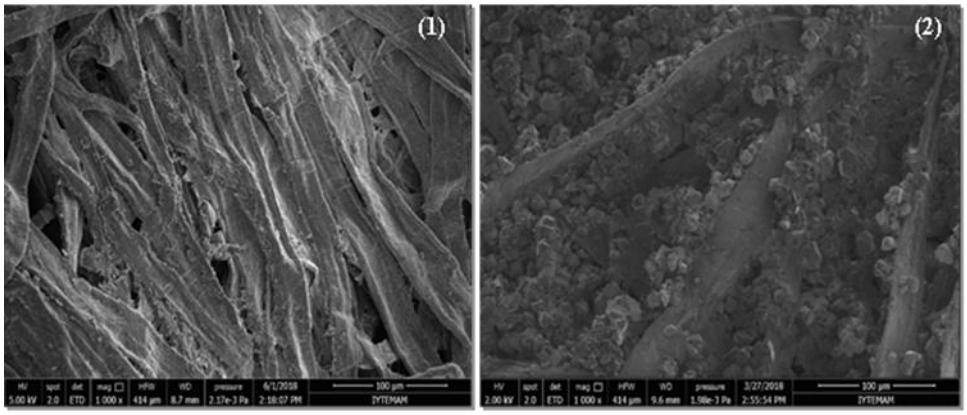

Figure 4. 2. Scanning electron micrograph (SEM) of long pulp fibers (1) and Cu-BTC deposited long pulp fibers (2).

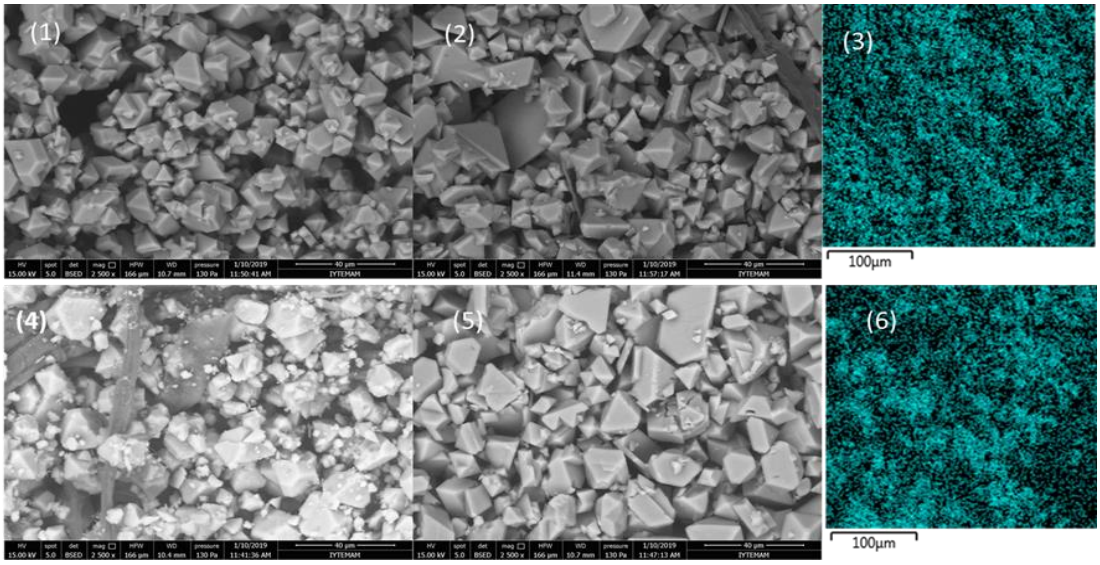

Figure 4. 3. Cu-BTC deposited short pulp fibers by stirring (1), non-stirring (2). Cu-BTC deposited long pulp fibers by stirring (4), non-stirring (5). Mapping analysis of Cu-BTC deposited on (3), long fibers (6). (period of time:12).

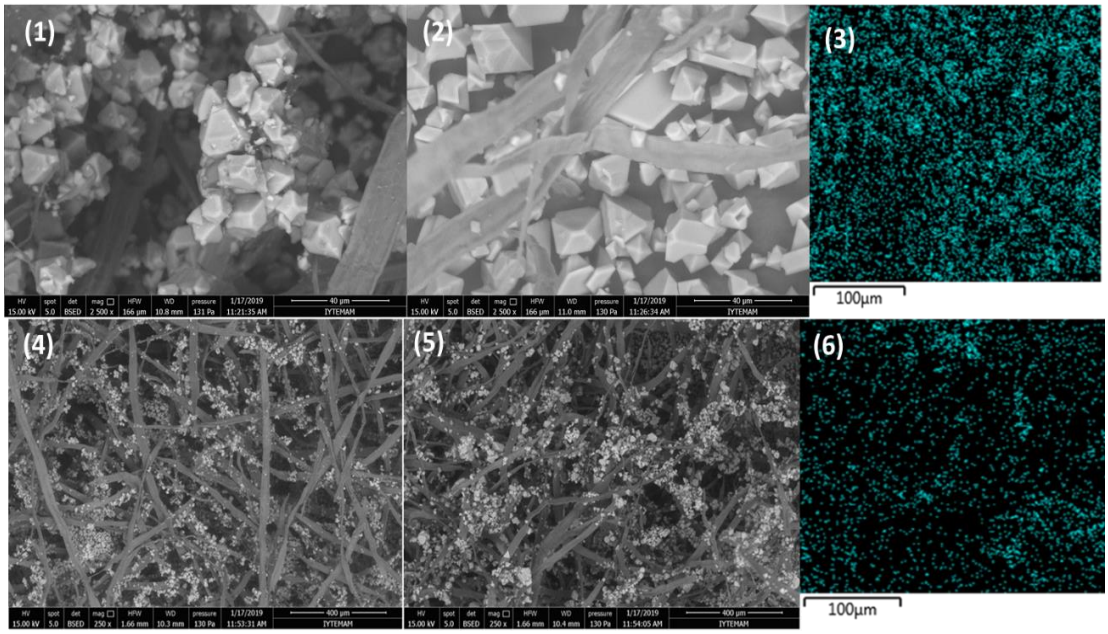

Figure 4. 4. Cu-BTC deposited long pulp fibers by stirring (1), non-stirring (2). Cu-BTC deposited long pulp fibers by stirring (4), non-stirring (5). Mapping analysis of Cu-BTC deposited on (3), long fibers (6).(period of time:12).

In order to investigate whether the deposition of Cu-BTC on short and long pulp fabrics was successfully achieved or not, the FT-IR analysis was carried out. While FT-IR spectra of Cu-BTC, raw short pulp fibers, and Cu-BTC deposited short pulp fibers which were synthesized by stirred and non-stirred method at 160 °C are represented in Figure 4. 5, FT-IR spectra of Cu-BTC, raw long pulp fibers and Cu-BTC deposited long pulp fibers which were synthesized by stirred and non-stirred method at 160 °C are represented in Figure 4. 6.

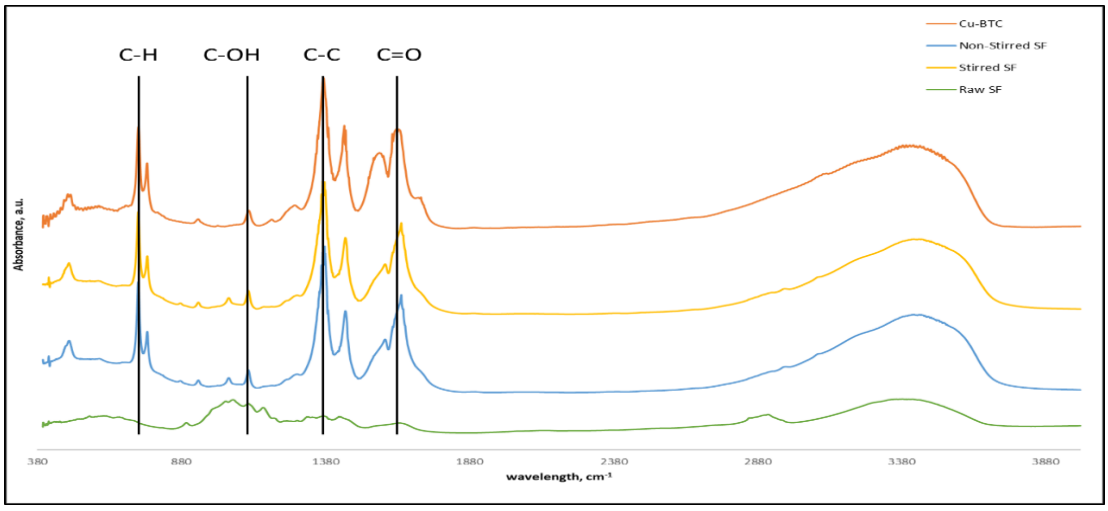

Figure 4. 5. FT-IR spectra of Cu-BTC, raw and Cu-BTC deposited short pulp fibers at 160 °C.

In Figure 4. 5., while the characteristic peaks of Cu-BTC are observed around 1600 cm^{-1}, 1400 cm^{-1}, 1300 cm^{-1}, and 730 cm^{-1}, raw short pulp fibers give their characteristic peaks around 1100 cm^{-1}, 2700 cm^{-1}, and 3200 cm^{-1}. The characteristic peaks of Cu-BTC were observed at the same wavelength in different studies which were carried out by Pinto et al. and Neufeld et al. (Pinto et al. (2012); Neufeld et al. (2015)). After the deposition of Cu-BTC on the short pulp fibers by stirring or non-stirring method, the intensities of peaks at 1644 cm^{-1}, 1447 cm^{-1}, 1343 cm^{-1}, and 729 cm^{-1} increased.

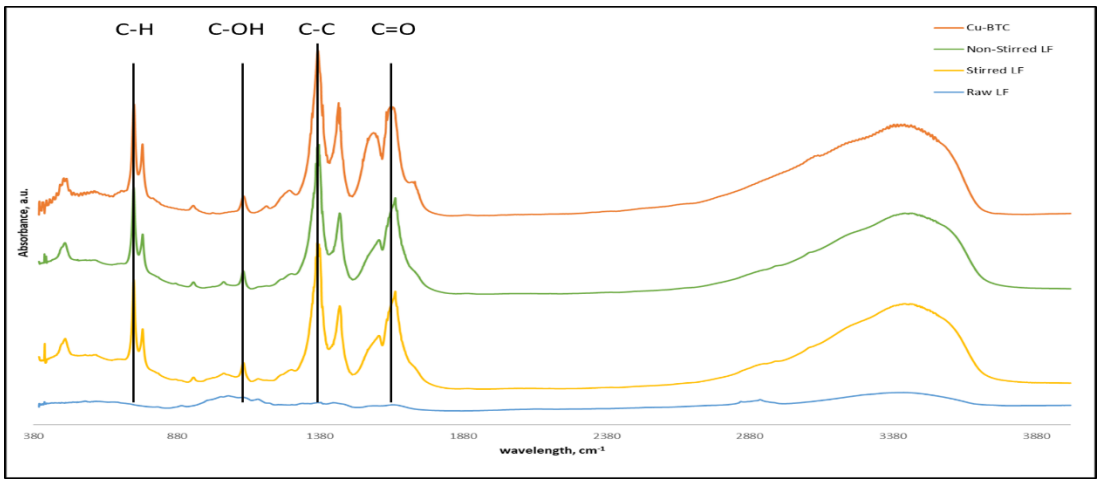

Figure 4. 6. FT-IR spectra of Cu-BTC, raw and Cu-BTC deposited long pulp fibers at 160 °C.

The COO− asymmetric bond, C−C stretches, COO− symmetric stretching, and C−H out-of-plane bending for Cu-BTC are observed at 1644 cm^{-1}, 1447 cm^{-1}, 1343 cm^{-1}, and 729 cm^{-1}, respectively. These characteristic peaks of Cu-BTC were observed at the same wavelength in the studies carried out by Pinto et al. and Neufeld et al. (Pinto et al. (2012); Neufeld et al. (2015)). Figure 4. 5. and Figure 4. 6. shows raw short and long pulp fibers give their selulosic characteristic peaks around 1100 cm^{-1}, 2700 cm^{-1}, and 3200 cm^{-1} and the Cu-BTC was succesifully deposited on the short and long pulp fibers by stirring or non-stirring method. It can be concluded that the intensity of the characteristic peaks of raw long pulp fibers increased after the Cu-BTC deposition (Pinto et al. (2012); Neufeld et al. (2015)).

The Cu-BTC deposited short fibers were synthesized by stirring and non-stirring methods at 85 °C and 160 °C. While the FT-IR analysis of Cu-BTC deposited short fibers, which were synthesized by stirring is given in Figure 4. 7., the FT-IR analysis of Cu-BTC deposited long fibers which were synthesized by stirring is given in Figure 4. 8.

There is not much difference between the intensity of characteristic peaks of Cu-BTC deposited short and long fibers, which were synthesized at 160 °C and 85 °C, so it could be concluded that the increase of temperature does not have a negative effect on the deposition of Cu-BTC.

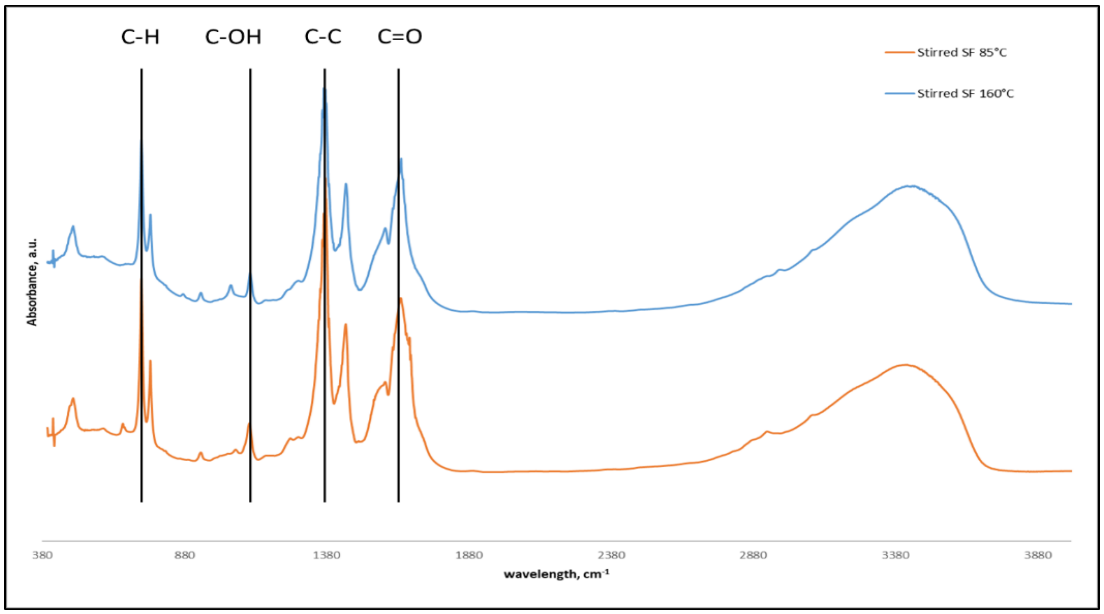

Figure 4. 7. FT-IR spectra of Cu-BTC deposited short pulp fibers by stirring at 160 °C and 85 °C.

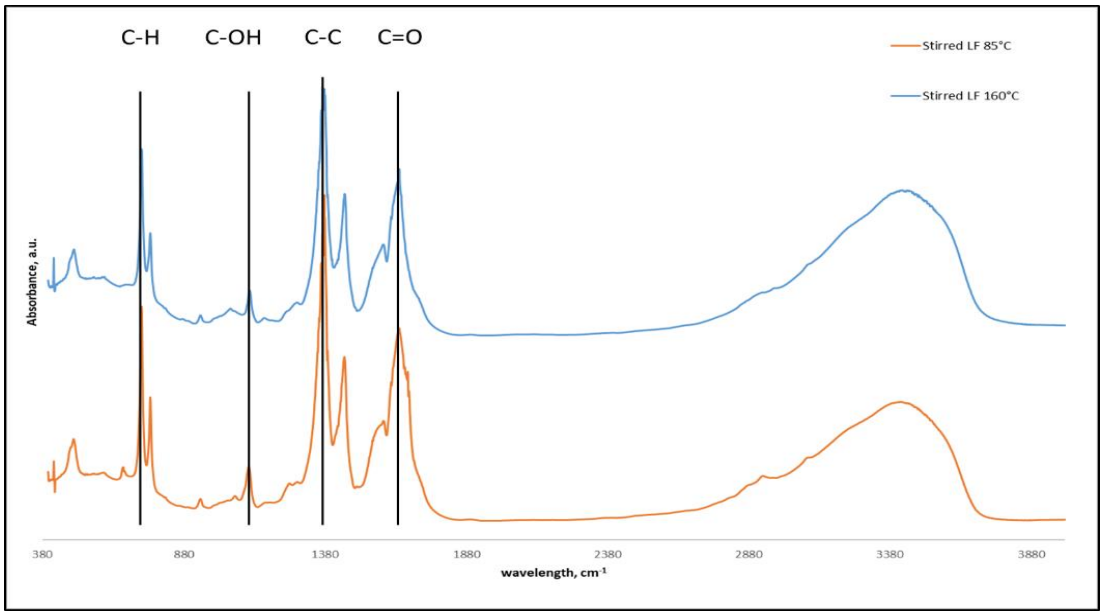

Figure 4. 8. FT-IR spectra of Cu-BTC deposited LF by stirring at 160 °C and 85 °C.

ATR-IR analysis was carried out for Cu-BTC, raw short pulp fibers and Cu-BTC deposited short pulp fibers and the results are given in Figure 4. 9. Besides, it was performed for Cu-BTC, raw long pulp fibers and Cu-BTC deposited long pulp fibers and the results are given in Figure 4. 10.

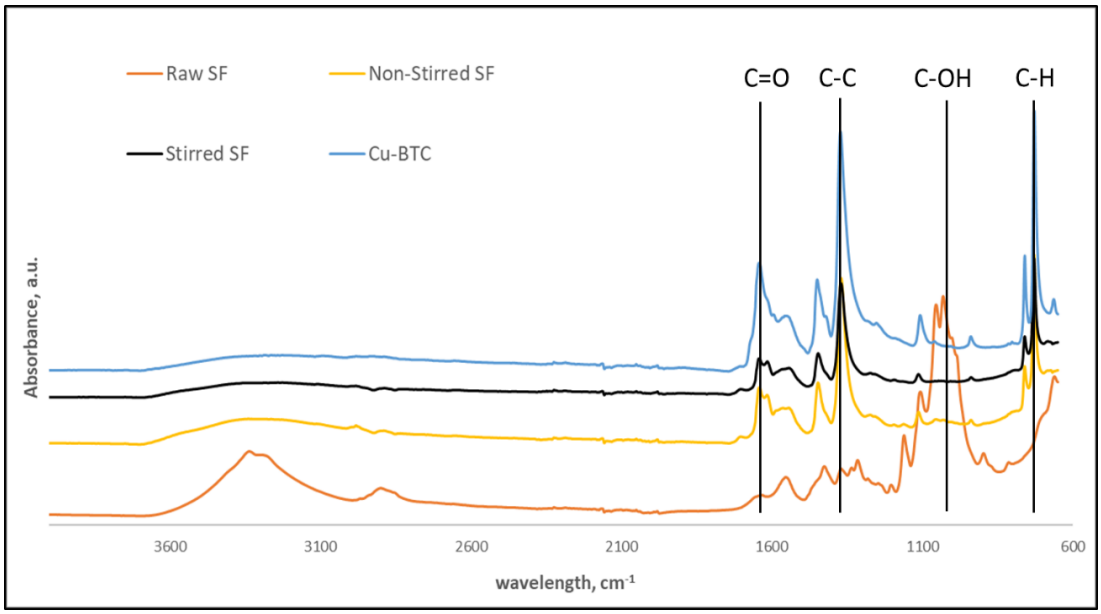

Figure 4. 9. ATR-IR spectra of Cu-BTC, raw and Cu-BTC deposited SF at 160 °C.

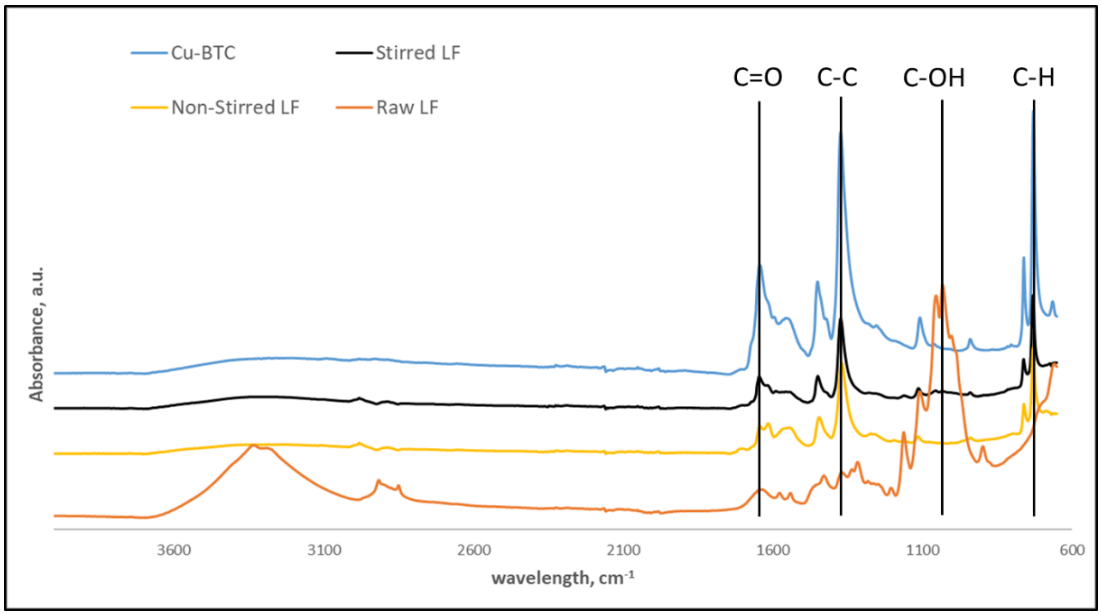

Figure 4. 10. ATR-IR spectra of Cu-BTC, raw and Cu-BTC deposited long pulp fibers at 160 °C.

The characteristic peaks of Cu-BTC, raw short pulp fibers, and Cu-BTC deposited short and long pulp fibers were observed at 728, 1371 and 1644 cm^{-1}. The results are similar to the FT-IR results of them. After the deposition of Cu-BTC, the place of the characteristic peaks was drifted slightly.

The effect of depostion time on the amount of deposited Cu-BTC on long and pulp fibers were investigated at three different deposition time (6 h, 12 h and 24 h). The results

are given in Figure 4. 11., Figure 4. 12., Figure 4. 13., and Figure 4. 14.. The optimum depostion time was chosen as 12 hours for the all of them.

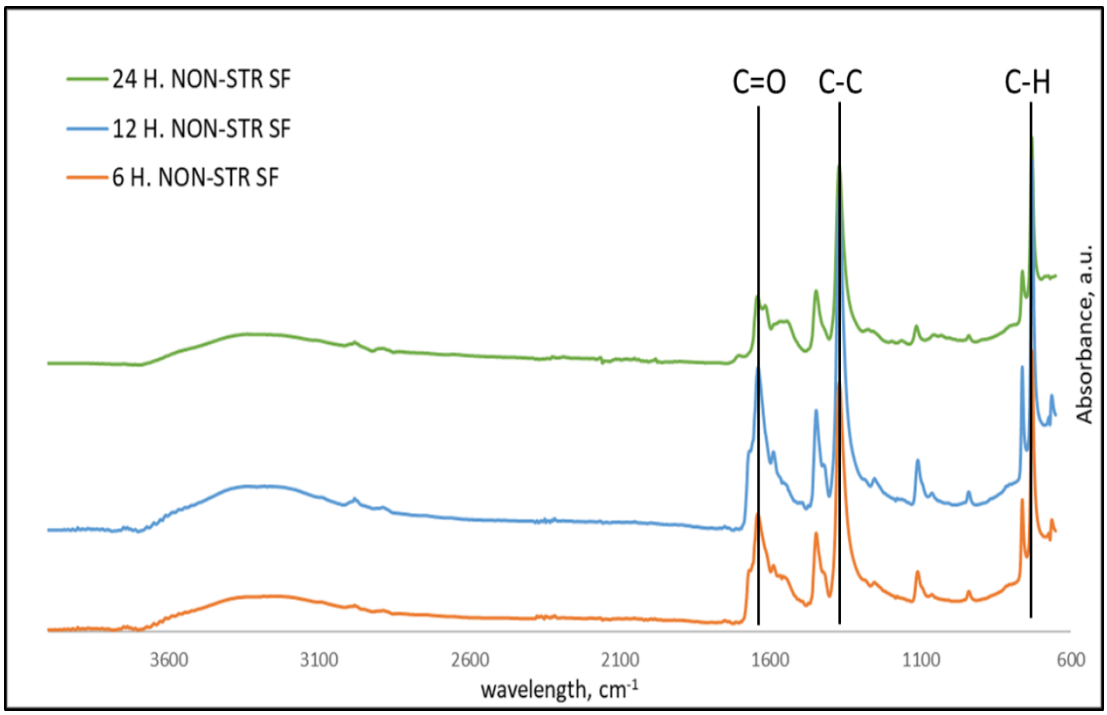

Figure 4. 11. ATR-IR spectra of non-stirred Cu-BTC deposited short pulp fibers at 160 °C with different deposition times.

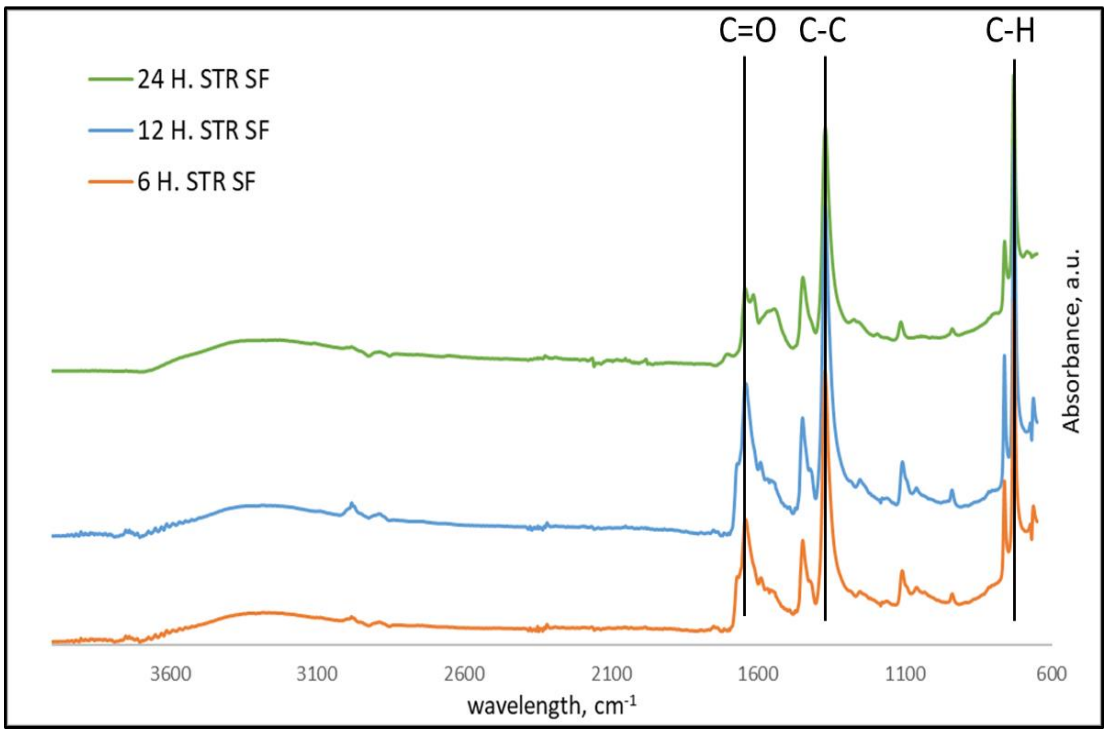

Figure 4. 12. ATR-IR spectra of stirred Cu-BTC deposited short pulp fibers at 160 °C with different deposition times.

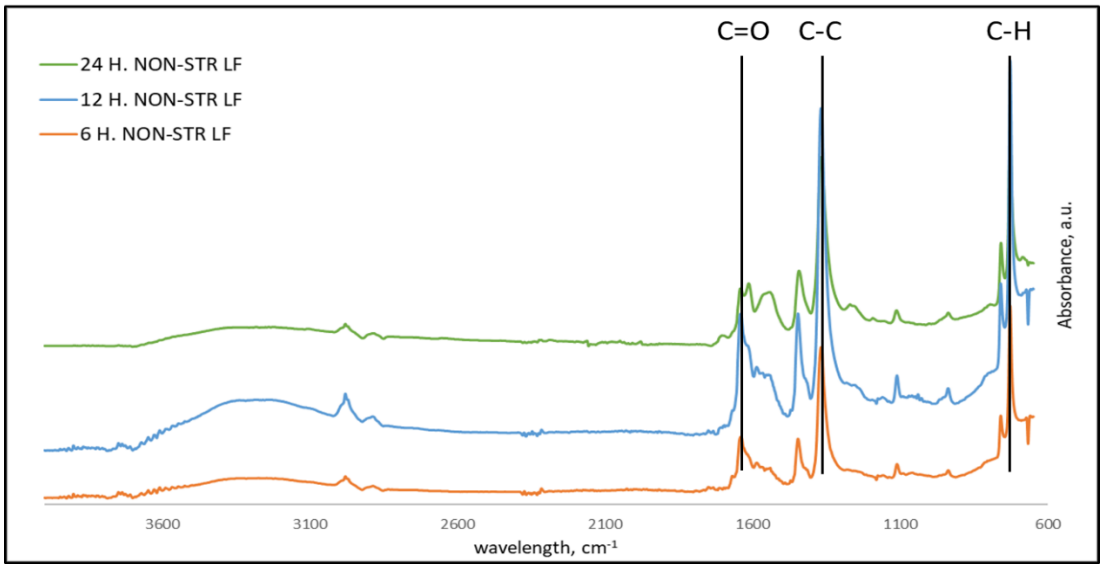

Figure 4. 13. ATR-IR spectra of non-stirred Cu-BTC deposited long pulp fibers at 160 °C with different deposition times.

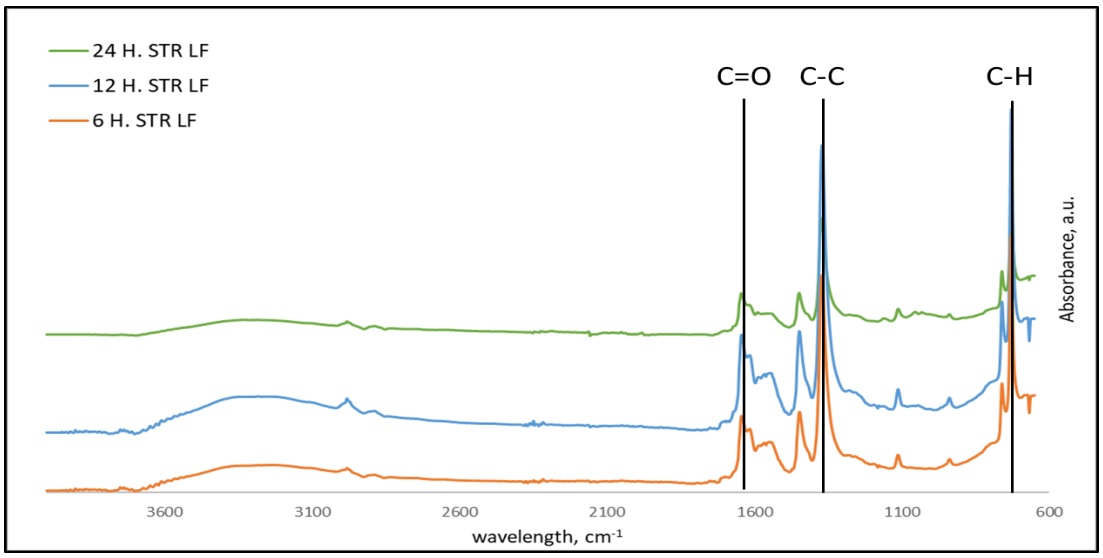

Figure 4. 14. ATR-IR spectra of stirred Cu-BTC deposited long pulp fibers at 160 °C with different deposition times.

While the XRD pattern of Cu-BTC, raw short pulp fibers, and Cu-BTC deposited short pulp fibers which were synthesized by stirred and non-stirred at 160 °C are shown in Figure 4. 15., the XRD pattern of Cu-BTC, raw long pulp fibers and Cu-BTC deposited long pulp fibers which were synthesized by stirred and non-stirred at 160 °C are shown in Figure 4. 16. It could be concluded that short and long pulp fibers has an amorphous structure according to the XRD results. Neufeld et al. found that the characteristic diffraction peaks associated with Cu-BTC are at 7.8, 9.5, 12, 13.5, 15, 17.8, and 19.3° (Neufeld et al., 2015).

The same characteristic peaks for Cu-BTC and Cu-BTC deposited short pulp fibers which were synthesized by stirring and non-stirring at 160 °C. Consequently, it could be deduced from this pattern, the deposition of Cu-BTC on short pulp fibers was successfully achieved by stirring and non-stirring method at 160 °C.

The characteristic peaks of Cu-BTC are clearly observed at 7.8, 9.5, 12, 13.5, 15, 17.8, and 19.3 degrees in Figure 4. 16. The intensity of these peaks increased after the deposition on the surface of long pulp fibers, however, there is not significant increase between the Cu-BTC deposited long and short fibers. Thus, it implies that the length of the pulp fibers do not have an importance on the deposition of Cu-BTC on their surface.

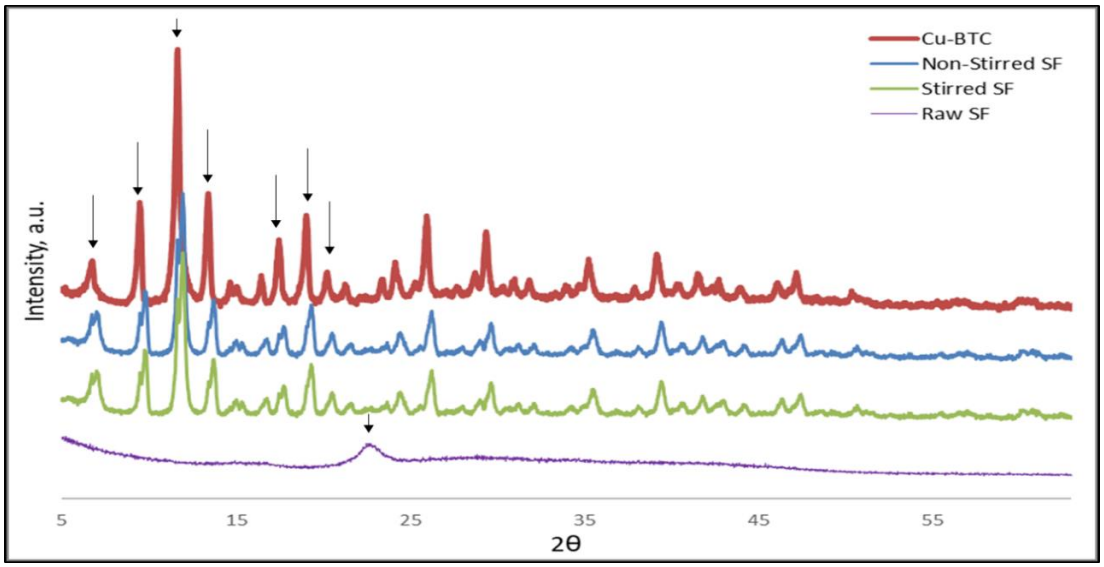

Figure 4. 15. XRD pattern of Cu-BTC, raw and Cu-BTC deposited short pulp fibers at 160 °C.

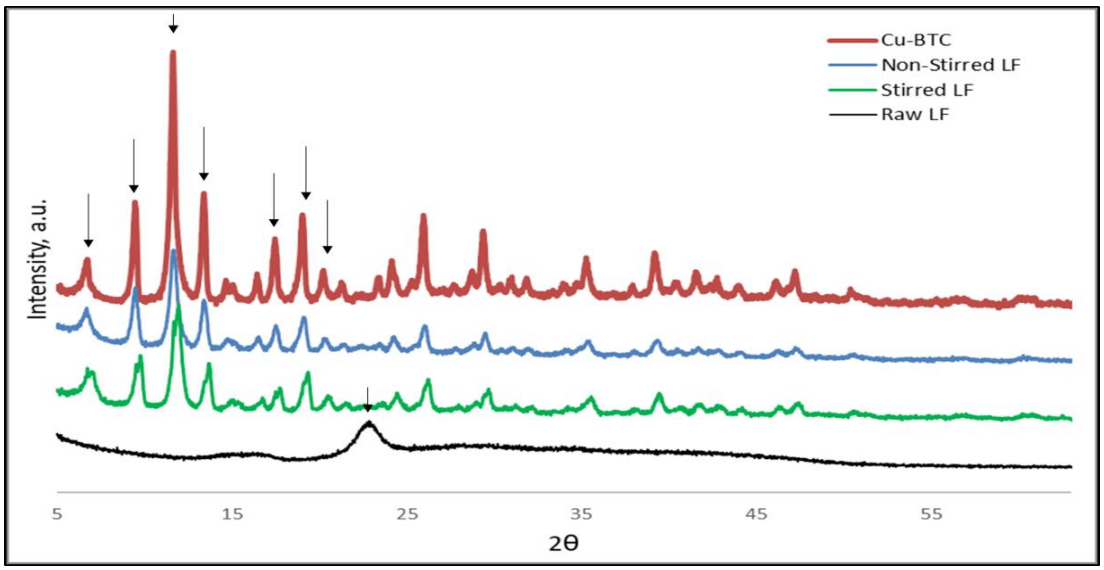

Figure 4. 16. XRD pattern of Cu-BTC, raw and Cu-BTC deposited long pulp fibers at 160 °C.

XRD patterns of non-stirred and stirred Cu-BTC deposited short pulp fibers at 160 °C and different deposition times are given in Figure 4. 17 and Figure 4. 18, respectively. Figure 4. 17. show that different deposition times are effective on the deposited amount of Cu-BTC. According to the results, the highest intensities were observed when the deposition time was 12 hours so it could be concluded that the optimum deposition time was selected as 12 hours for this study. According to Figure 4. 18., the deposition time does not have a significant effect on the amount of deposited Cu-BTC. Additionally, the amount of deposited Cu-BTC by non-stirring was higher than the amount of deposited Cu-BTC by stirred.

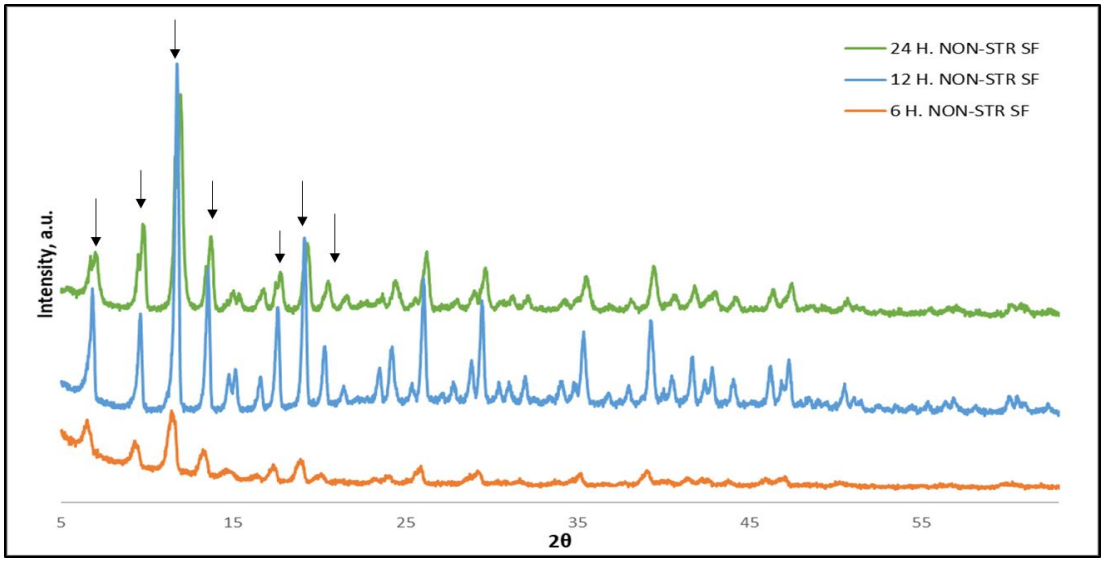

Figure 4. 17. XRD pattern of non-stirred Cu-BTC deposited short pulp fibers at 160 °C and different deposition times.

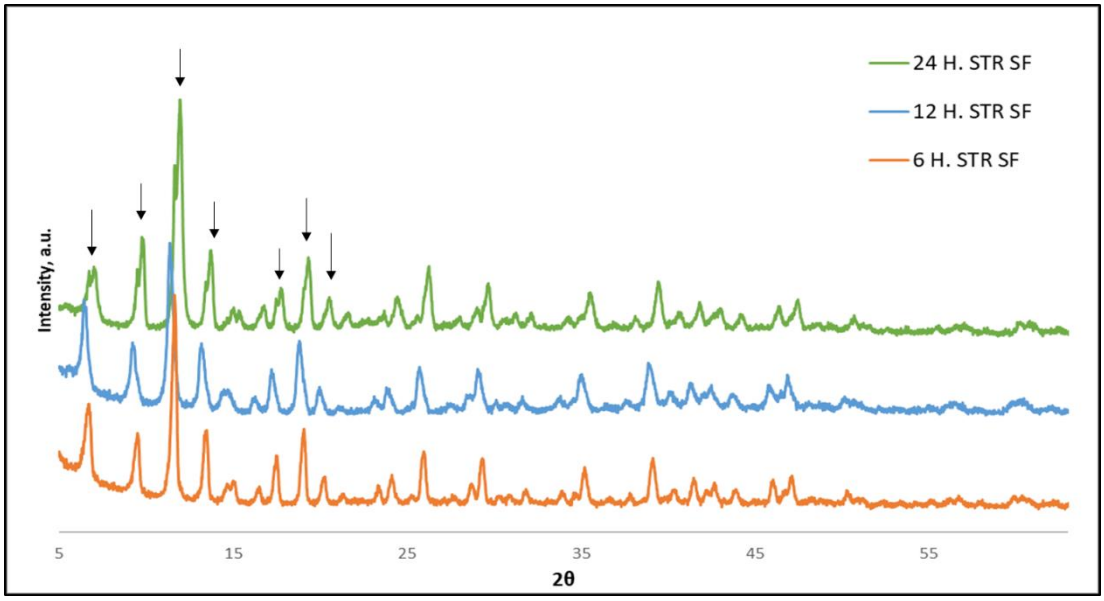

Figure 4. 18. XRD pattern of stirred Cu-BTC deposited short pulp fibers at 160 °C and different deposition times.

XRD patterns of non-stirred and stirred Cu-BTC deposited long pulp fibers at 160 °C and different deposition times are given in Figure 4. 19 and Figure 4. 20, respectively. The highest deposited amount of Cu-BTC by non-stirring was obtained at 6 hours. The longer deposition times does not provide an increase in the deposited Cu-BTC amount. Additionally, 6 hours and 12 hours are almost the same deposited Cu-BTC amount by stirring. Consequently, 6 hours are enough for the deposition of Cu-BTC on the long fibers either stirring or non-stirring.

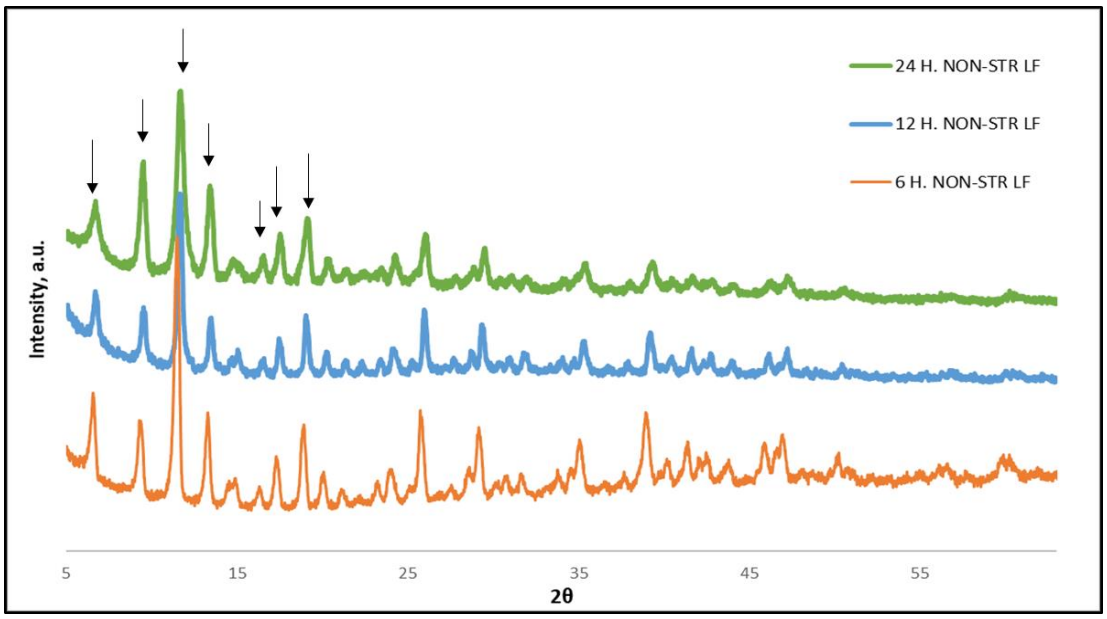

Figure 4. 19. XRD pattern of non-stirred Cu-BTC deposited long pulp fibers at 160 °C and different deposition times.

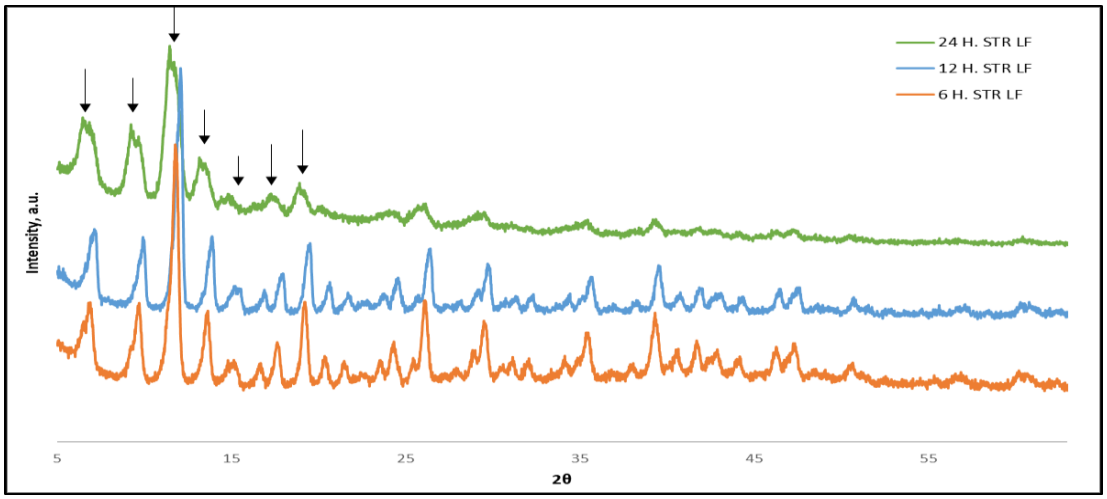

Figure 4. 20. XRD pattern of stirred Cu-BTC deposited long pulp fibers at 160 °C and different deposition times.

NH_3 sensing properties of Cu-BTC deposited short and long pulps were investigated and the results are given in Figure 4. 21.

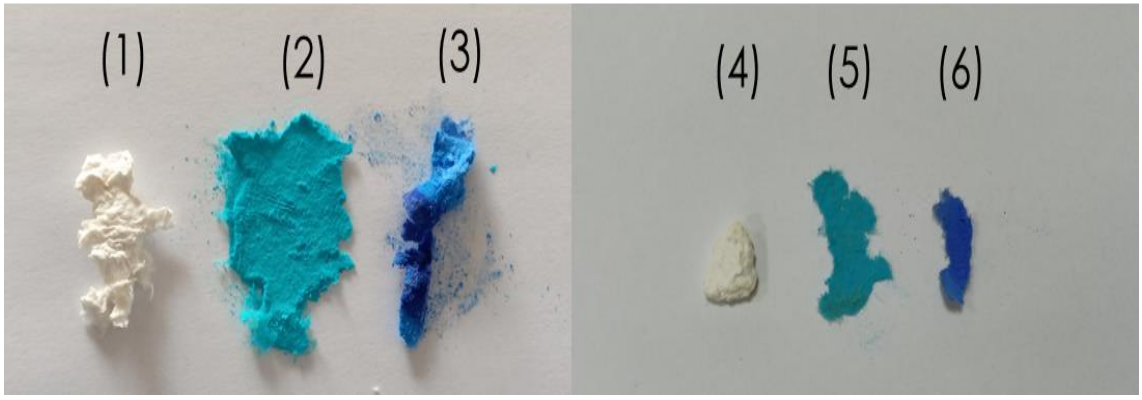

Figure 4. 21. Raw short pulp (1), Cu-BTC deposited short pulp (2), NH_3 exposed Cu-BTC deposited short pulp (3), raw long pulp (4), Cu-BTC deposited long pulp (5), NH_3 exposed Cu-BTC deposited long pulp (6).

After the Cu-BTC deposited short and long pulps had exposed to NH_3 gas, their color were changed since NH_3 was bonded with copper ions. Consequently, Cu-BTC deposited short and long pulps have NH_3 sensing property.

4.2. Characterization Study of Raw and Cu-BTC Deposited Cotton

In order to investigate the feature of raw cotton fabric and Cu-BTC deposited cotton fabric, SEM analysis was carried out with 1000x magnification and hence the results of this analysis are given in Figure 4. 22..

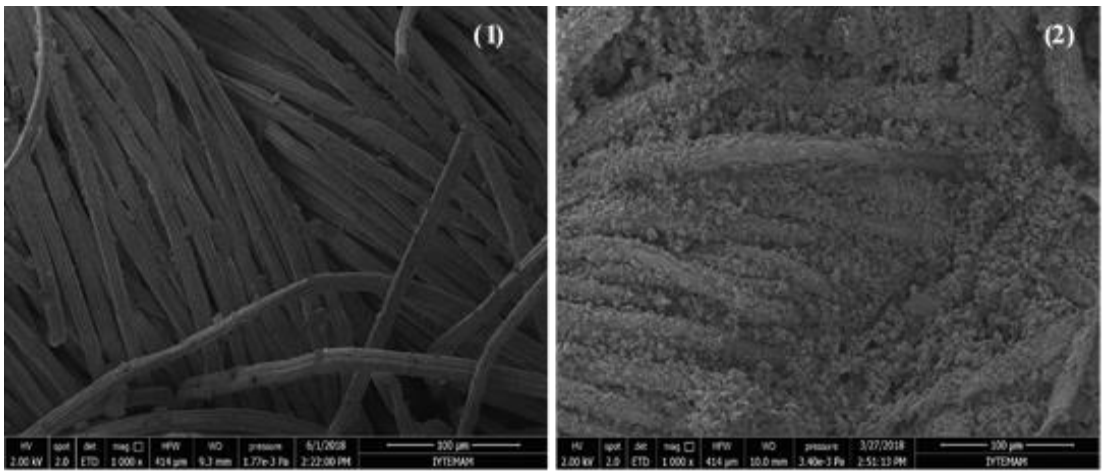

Figure 4. 22. SEM micrographs of the cotton fabric (1) and Cu-BTC deposited cotton fabric (2).

According to Figure 4. 22.(1), the raw cotton fabrics have a long and thin stripe shape, and Figure 4. 22.(2), shows that Cu-BTC is successfully deposited on cotton

fabrics. It is clearly seen that Cu-BTC crystals are orderly distributed along the cotton fabrics. Additionally, the surface of the cotton fabric is intensely covered with Cu-BTC crystals. Similar features were observed in the study of Pinto et al. It could be concluded that Cu-BTC was successfully synthesized and deposited on the surface of cotton fabrics (Pinto et al., 2012).

The effect of deposition cycle number for second method on the amount of deposited Cu-BTC on cotton fabrics was investigated and the SEM micrograhs of 5, 10 and 15 cycles are given in Figure 4. 23.

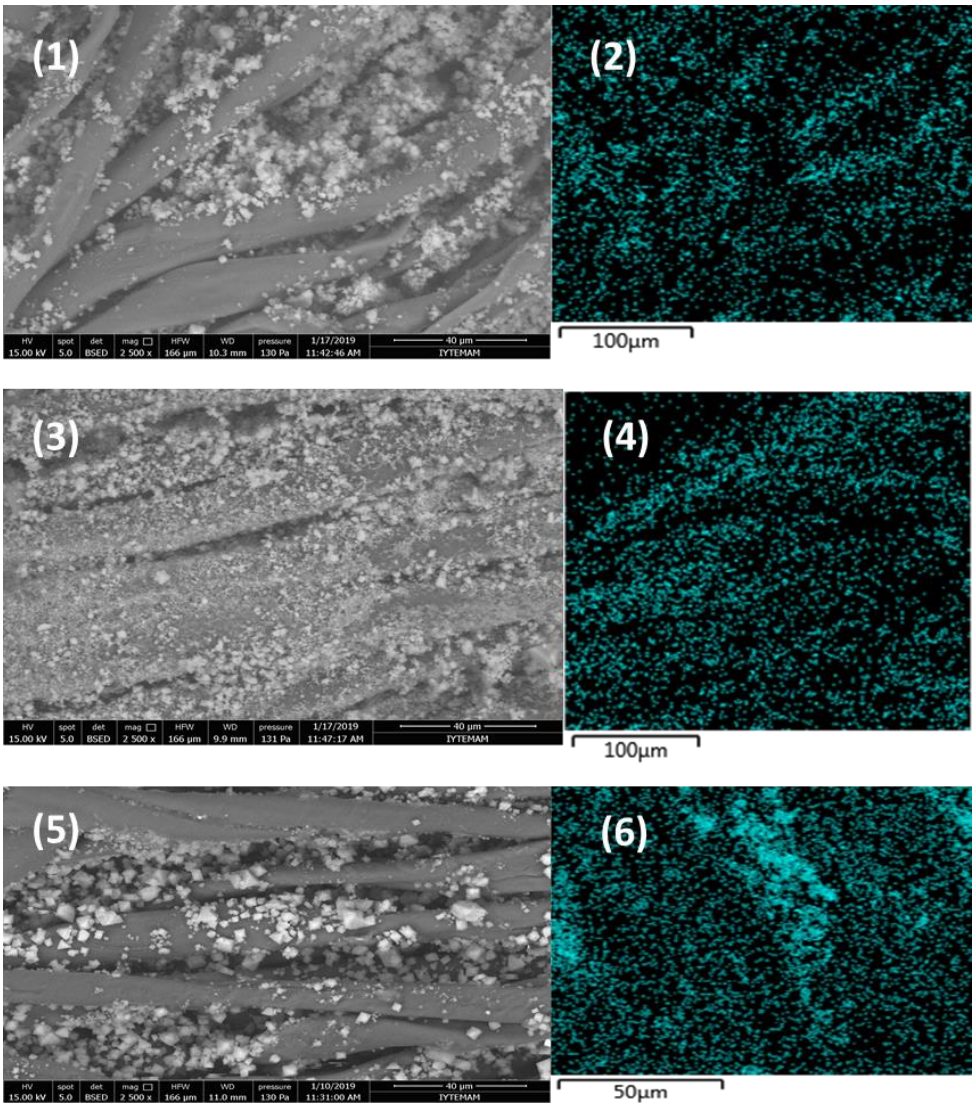

Figure 4. 23. Cu-BTC deposited cotton fabric, 5 cycle (1), mapping analysis of Cu-BTC deposited on cotton fabrics for 5 cycle (2), Cu-BTC deposited cotton fabric, 10 cycle (3), mapping analysis of Cu-BTC deposited on cotton fabrics for 10 cycle (4), Cu-BTC deposited cotton fabric, 15 cycle (5), mapping analysis of Cu-BTC deposited on cotton fabrics for 15 cycle (6).

Cu-BTC deposited on the surface of cotton fabric was successfully achieved by second deposition method for all cycle numbers. However, applying 10 cycles give better result than 5 and 15 cycles, almost all surface of cotton fabric was covered by with 10 cycles. Thus, optimum cycle number could be chosen as 10 for Cu-BTC deposition on cotton fabric.

The effect of deposition cycle number for third method on the amount of deposited Cu-BTC on cotton fabrics was investigated and the SEM micrograhs of 4, 8 and 12 cycles are given in Figure 4. 24.

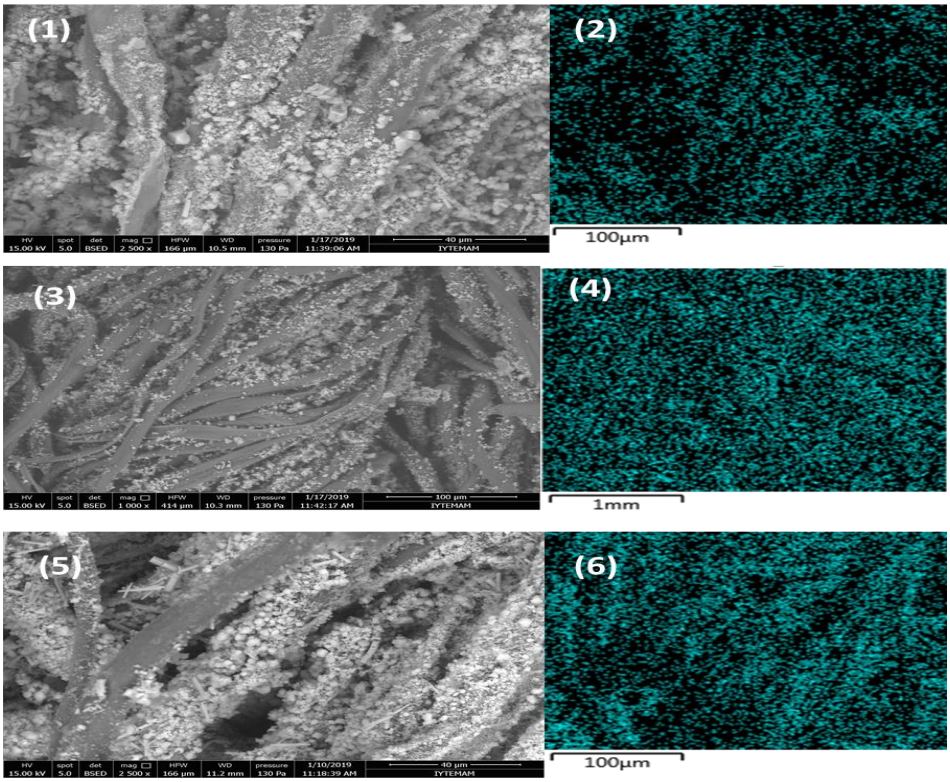

Figure 4. 24. Cu-BTC deposited cotton fabric, 4 cycle (1), mapping analysis of Cu-BTC deposited on cotton fabrics for 4 cycle (2), Cu-BTC deposited cotton fabric, 8 cycle (3), mapping analysis of Cu-BTC deposited on cotton fabrics for 8 cycle (4), Cu-BTC deposited cotton fabric, 12 cycle (5), mapping analysis of Cu-BTC deposited on cotton fabrics for 12 cycle (6).

The surface of the cotton fabric was successfully covered with Cu-BTC by third deposition method for all cycle numbers. According to the results, optimum cycle number was chosen as 12 for third deposition method since a uniform Cu-BTC distribution and well-shaped Cu-BTC particles on the surface of cotton fabric were obviously seen.

In order to investigate whether the carboxymethylation process and the deposition of Cu-BTC on the surface of cotton were successfully achieved or not, FT-IR analysis is carried out. The FT-IR analysis results of raw cotton, Cu-BTC, carboxymethylated cotton fabric, and Cu-BTC deposited cotton fabric by three different methods are shown in Figure 4. 25., Figure 4. 26. and Figure 4. 27., respectively.

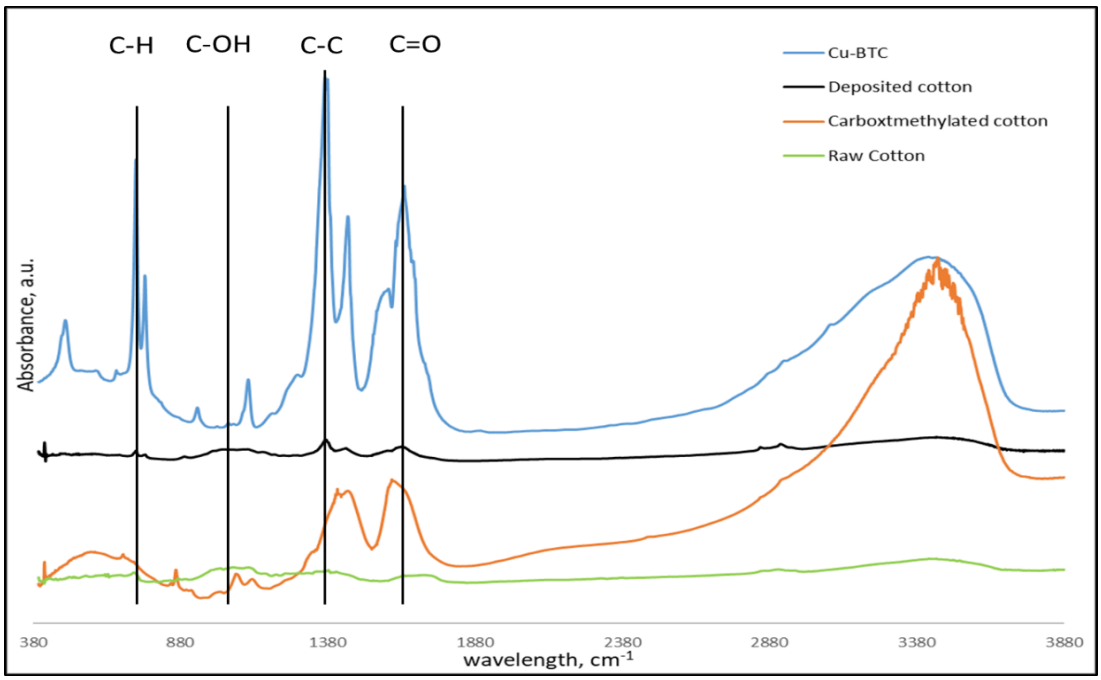

Figure 4. 25. FT-IR spectra of Cu-BTC, raw cotton, carboxymethylated cotton, and Cu-BTC deposited cotton by the first method.

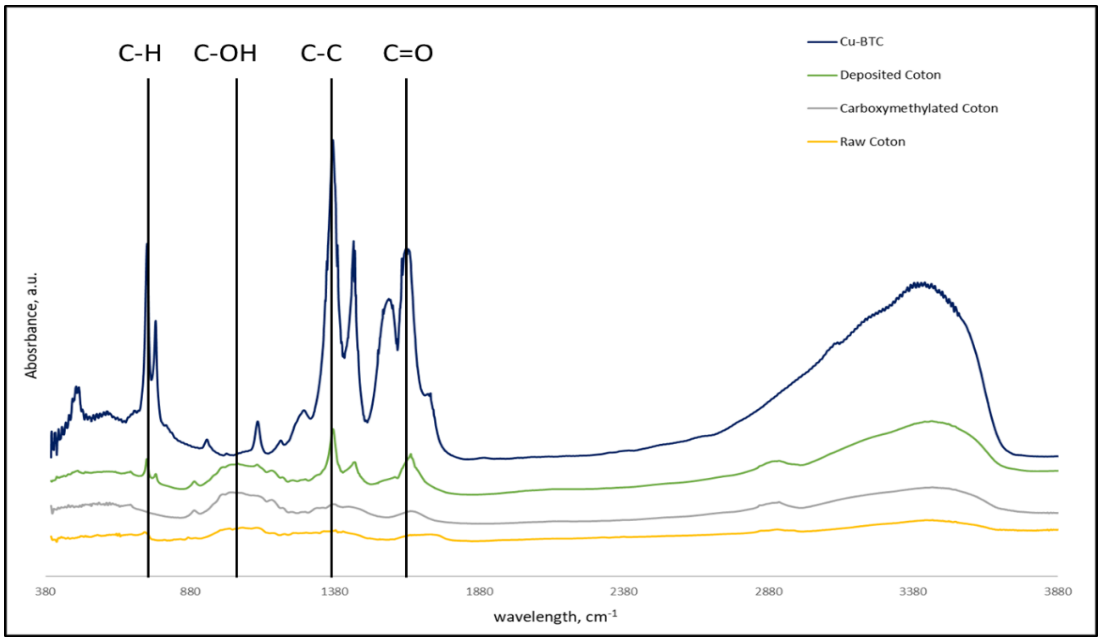

Figure 4. 26. FT-IR spectra of Cu-BTC, raw cotton, carboxymethylated cotton, and Cu-BTC deposited cotton by the second method.

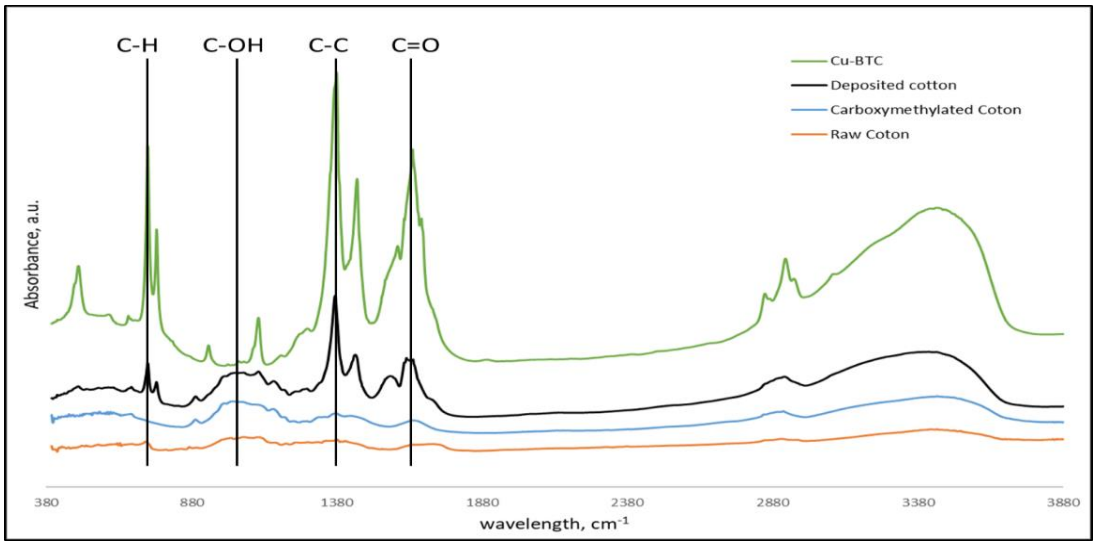

Figure 4. 27. FT-IR spectra of Cu-BTC, raw cotton, carboxymethylated cotton, and Cu-BTC deposited cotton by the third method.

According to the related figures, the characteristic peaks of cotton did not disappear after the carboxymethylation and deposition steps. Thus, the structure of cotton was preserved. Additionally, after the carboxymethylation step, similar results were obtained for both procedures so that there was not a significant difference between the carboxymethylation procedures to obtain carboxymethylated cotton fabrics. It can be concluded based on literature that the peak around 1645 cm^{-1} represents carboxylate groups and the peak around 2928 cm^{-1} represents C-H stretching so that the carboxymethylation was achieved successfully. After the carboxymethylation step, the intensity of C-H stretching and carboxylate groups peaks increased. The peaks around 728, 1371 and 1644 cm^{-1} refer to the Cu-BTC and the results of FT-IR spectra indicates that deposition of Cu-BTC on cotton has been achieved successfully. The similar IR results were obtained in two different studies which were about surface-anchored MOF-cotton material for tunable antibacterial copper delivery and Cu-BTC deposition on cotton (Rubin et al., 2018; Pinto et al., 2012).

ATR-IR analysis was carried out for Cu-BTC, raw cotton, carboxymethylated cotton, and Cu-BTC deposited cotton specimens with three different methods to investigate whether the carboxymethylation and deposition steps were successfully achieved or not. The results of this analysis are given in Figure 4. 28, Figure 4. 29 and Figure 4. 30.

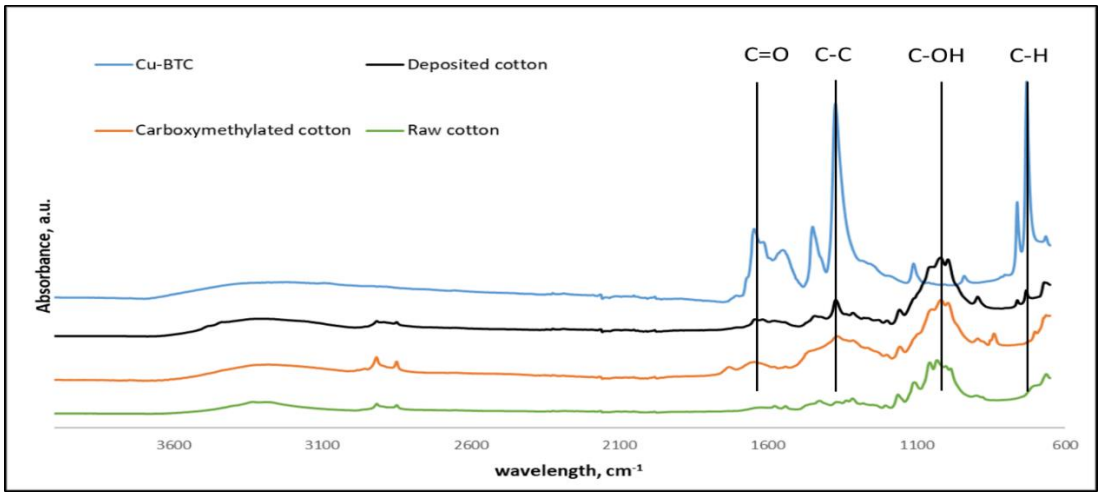

Figure 4. 28. ATR-IR spectra of the first method.

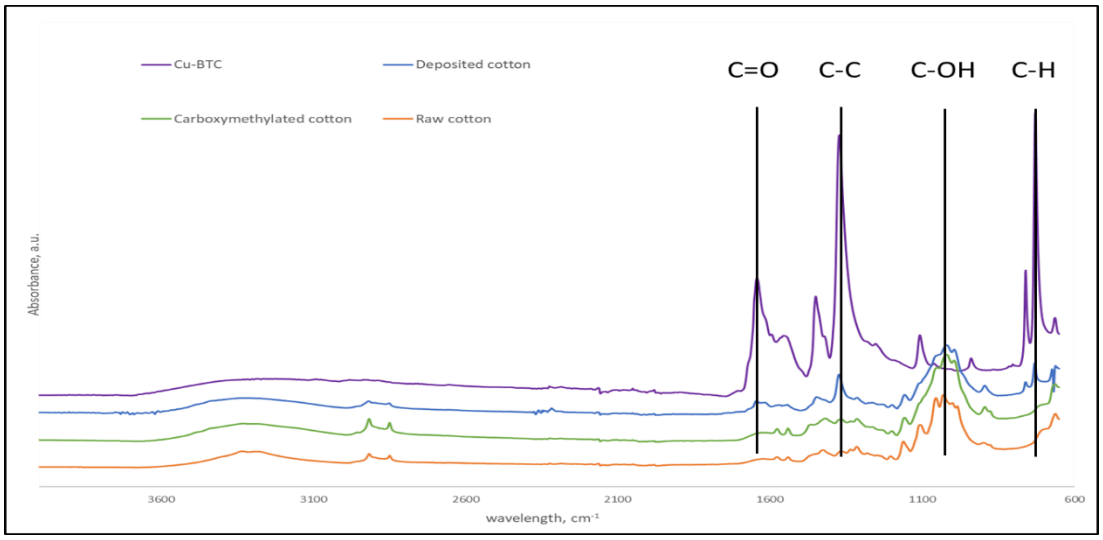

Figure 4. 29. ATR-IR spectra of the second method.

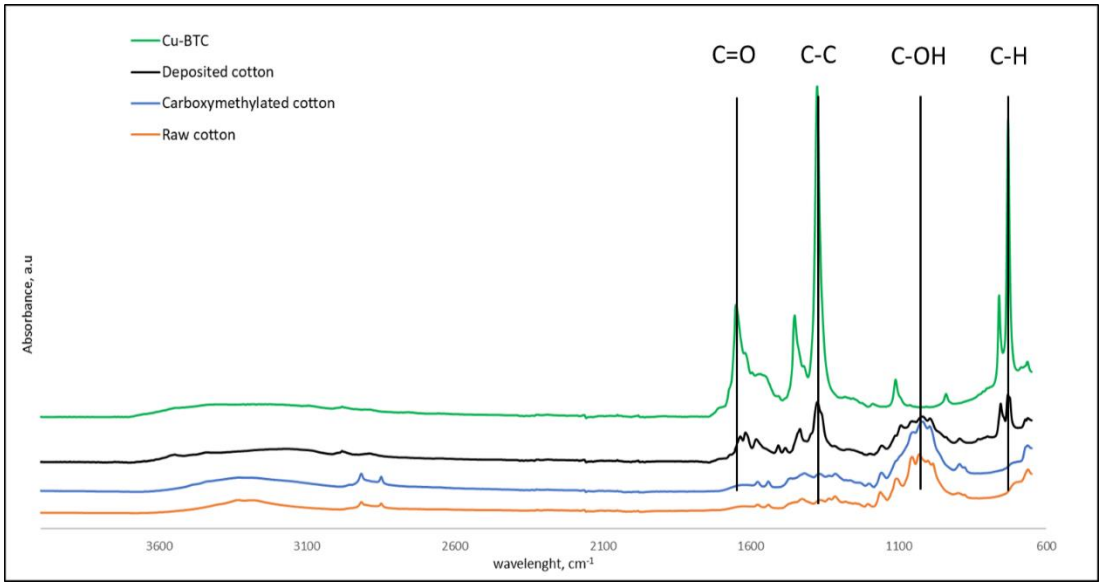

Figure 4. 30. ATR-IR spectra of the third method.

Neufeld et al. carried out a study over the Cu-BTC deposition onto the cotton fabric and ATR-IR analysis was performed to comprehend whether the deposition of Cu-BTC on the cotton fabric was successfully achieved or not in this study. The characteristic peaks of Cu-BTC, raw cotton, carboxymethylated cotton, and Cu-BTC deposited cotton specimens were observed at 728, 1371 and 1644 cm^{-1} (Neufeld et al., 2015). It could be deduced from the related figures that the carboxymethylation and deposition steps were successfully achieved. The characteristic peaks of Cu-BTC, raw cotton, carboxymethylated cotton, and Cu-BTC deposited cotton specimens were observed at 728, 1371 and 1644 cm^{-1}. After the deposition of Cu-BTC, the place of the characteristic peaks was drifted slightly. The results are similar with the study of Neufeld et al. so that the results are in accordance with the literature.

The effect of cycle number was investigated for the second and third method and the results are given in Figure 4. 31 and Figure 4. 32, respectively. According to the results, while the optimum cycle number for the second method was chosen as 10 and the optimum cycle number for the third method was selected as 12.

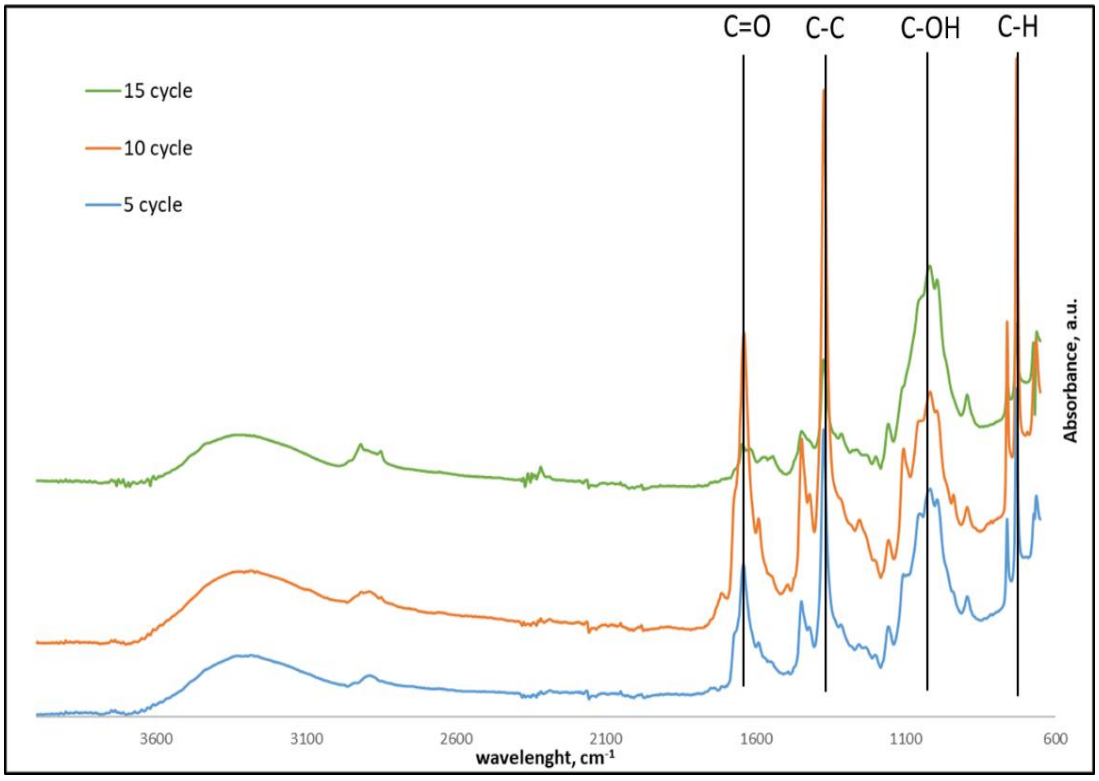

Figure 4. 31. ATR-IR spectra for the effect of cycle number on the deposition of Cu-BTC on cotton fabric for the second method

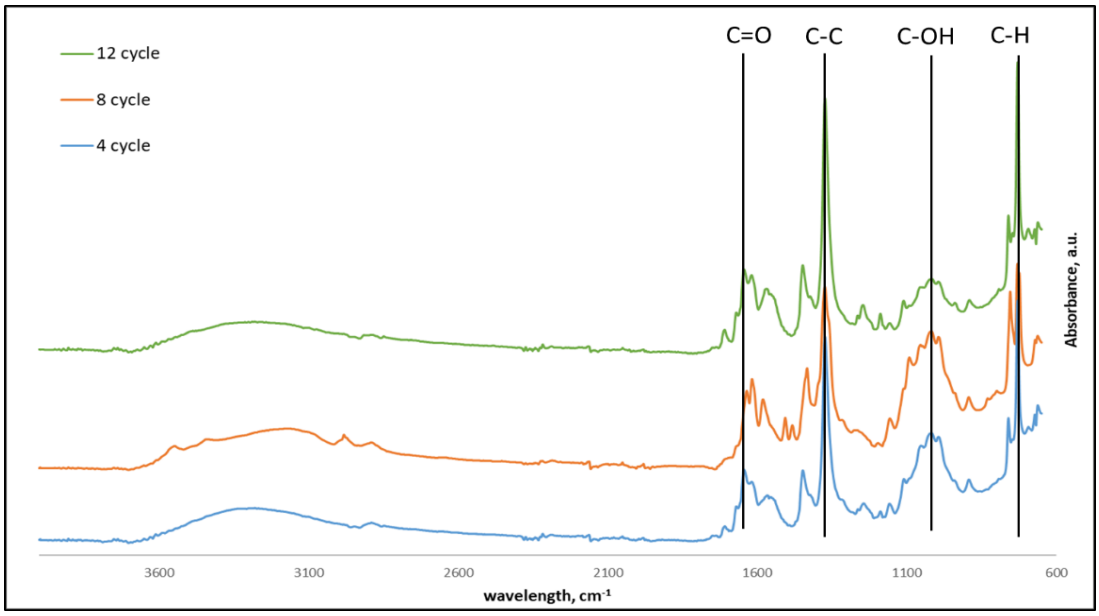

Figure 4. 32. ATR-IR spectra for the effect of cycle number on the deposition of Cu-BTC on cotton fabric for the second method.

The XRD patterns of Cu-BTC, raw cotton fabric and Cu-BTC deposited cotton fabric by different deposition methods are presented in Figure 4. 33, Figure 4. 34, and Figure 4. 35. Cotton has a characteristic peak around 23° and this peak was observed after all Cu-BTC deposition methods, the intensity of this peak decreased. Additionally, the place of this peak was drifted due to the interaction between the cotton surface and Cu-BTC. After the deposition process, new peaks, referred to the characteristic peaks of Cu-BTC, were observed. The intensities of characteristic peaks of Cu-BTC was observed weakly since Cu-BTC was deposited on the cotton surface as a thin layer. Thus, it could be said that the deposition process was successfully achieved by all deposition methods.

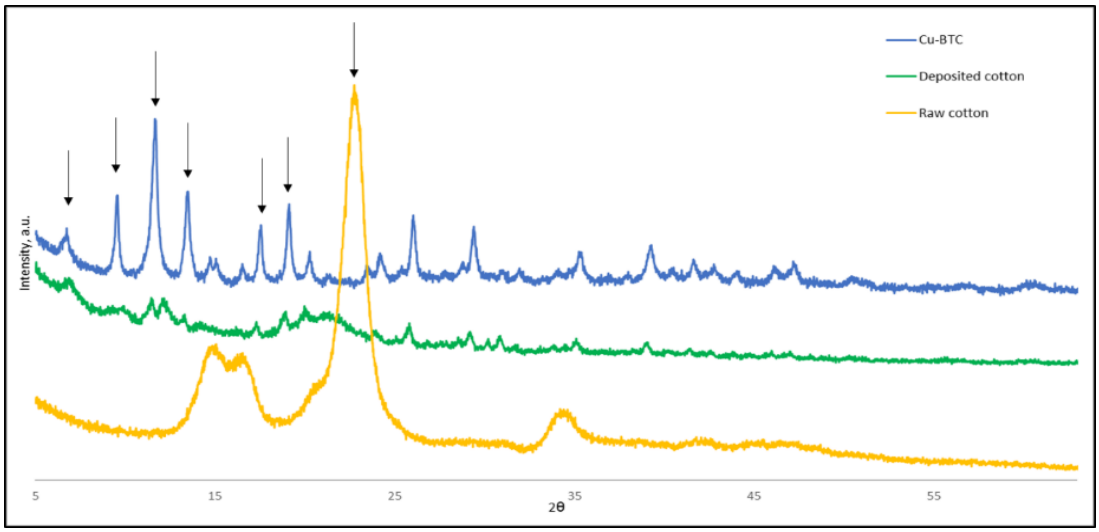

Figure 4. 33. XRD pattern of Cu-BTC, raw cotton fabric and Cu-BTC deposited cotton fabric (by first deposition method).

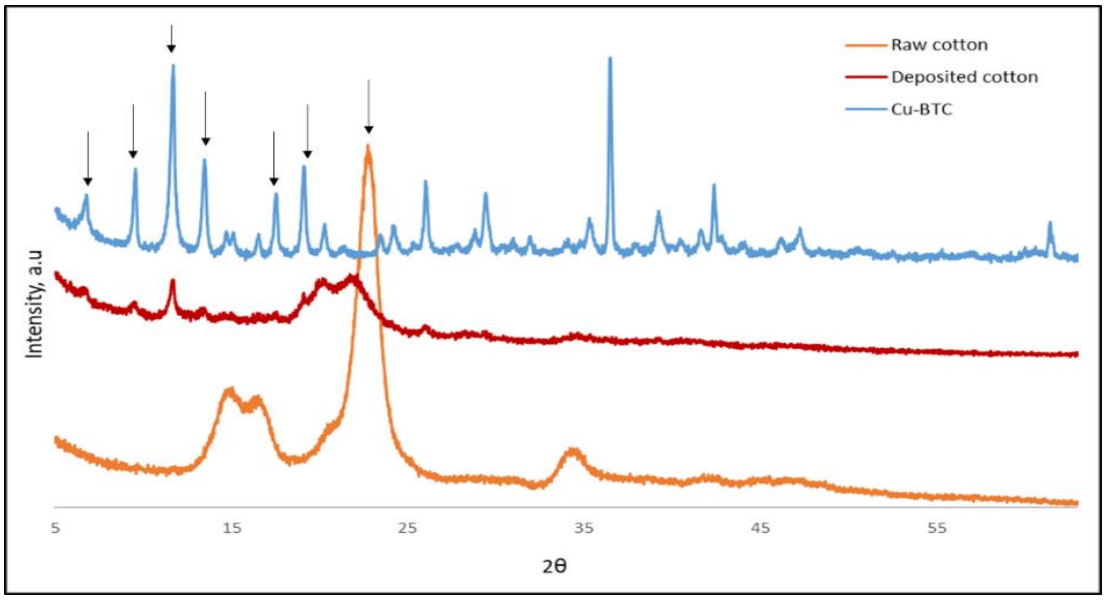

Figure 4. 34. XRD pattern of Cu-BTC, raw cotton fabric and Cu-BTC deposited cotton fabric (by second deposition method).

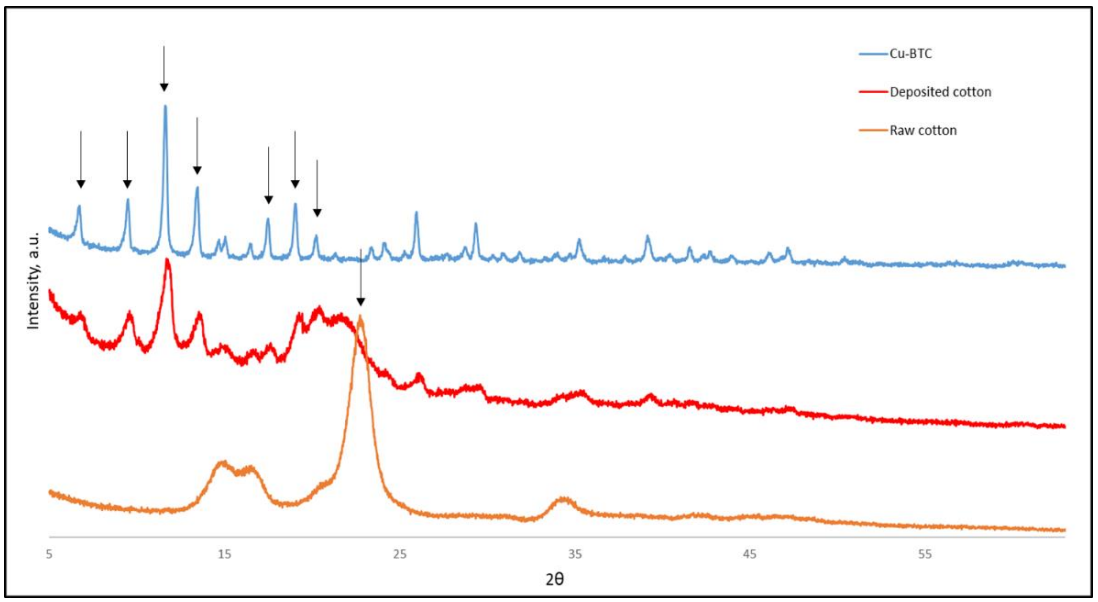

Figure 4. 35. XRD pattern of Cu-BTC, raw cotton fabric and Cu-BTC deposited cotton fabric (by third deposition method).

The effect of cycle number on the deposition of Cu-BTC on cotton fabric was investigated for the second and third deposition method. XRD results of them are given in Figure 4. 36 and Figure 4. 37. The deposition of Cu-BTC on cotton fabric was successfully achieved for second and third deposition method with different number of cycles. The XRD results are in accordance with the ATR-IR results. According to XRD results, 10 cycle for the second method and 12 cycle for the third method were chosen as optimum cycle numbers.

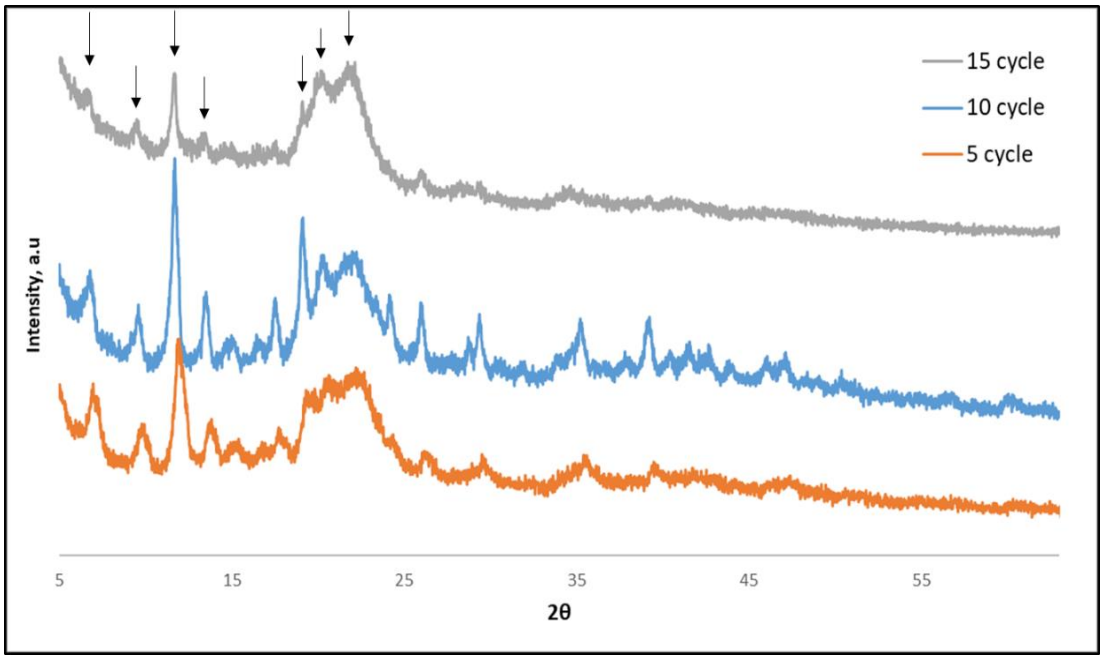

Figure 4. 36. XRD pattern for the effect of cycle number on the deposition of Cu-BTC on cotton fabric for the second method

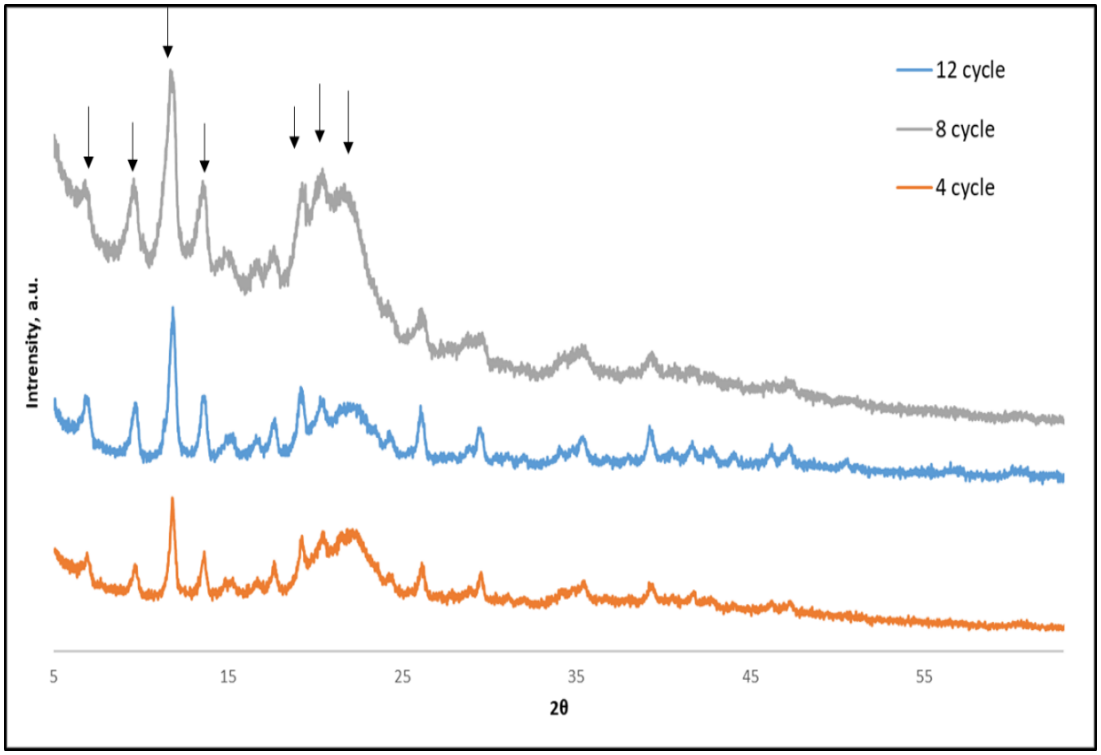

Figure 4. 37. XRD pattern for the effect of cycle number on the deposition of Cu-BTC on cotton fabric for the third method.

NH_3 sensing property of Cu-BTC deposited cotton fabric (by first method) was investigated and the results are shown in Figure 4. 38.

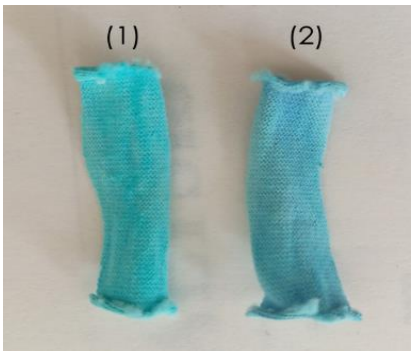

Figure 4. 38. Cu-BTC deposited cotton fabric (by first method) (1), NH_3 exposed Cu-BTC deposited cotton fabric (2).

After Cu-BTC deposited cotton fabric (by first method) exposed to NH_3, there is not a significant color change. Thus, this method is not appropriate to form Cu-BTC deposited cotton fabric which have NH_3 sensing property.

NH_3 sensing properties of Cu-BTC deposited cotton fabrics by second method and third method were investigated and the results are shown in Figure 4. 39. and Figure 4. 40., respectively.

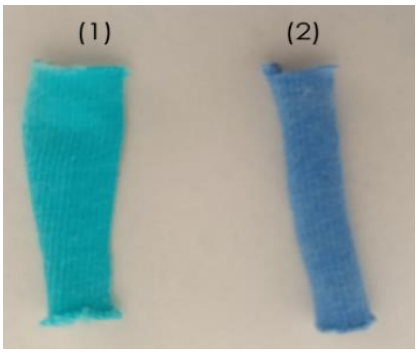

Figure 4. 39. Cu-BTC deposited cotton fabric (by second method) (1), NH_3 exposed Cu-BTC deposited cotton fabric (by second method) (2).

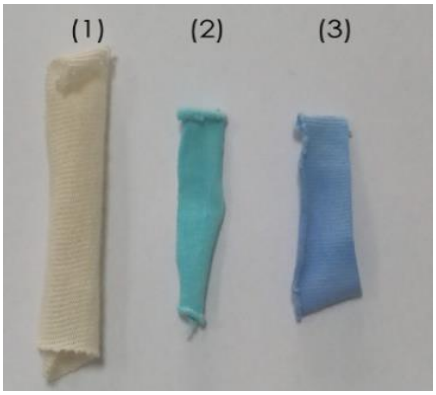

Figure 4. 40. Raw cotton fabric (1), Cu-BTC deposited cotton fabric (by third method) (2), NH_3 exposed Cu-BTC deposited cotton fabric (by third method) (3).

Cu-BTC deposited cotton fabrics by the second and third method have initially light blue color. After NH_3 exposure, Cu-BTC deposited cotton fabrics by the second and third method show a color change and their color turned to dark blue. Thus, they have NH_3 sensing property.

4.3. Characterization Study of Raw Viscose and Cu-BTC Deposited Viscose

The SEM results of raw viscose fabric, Cu-BTC deposited viscose fabric are given in Figure 4. 41.

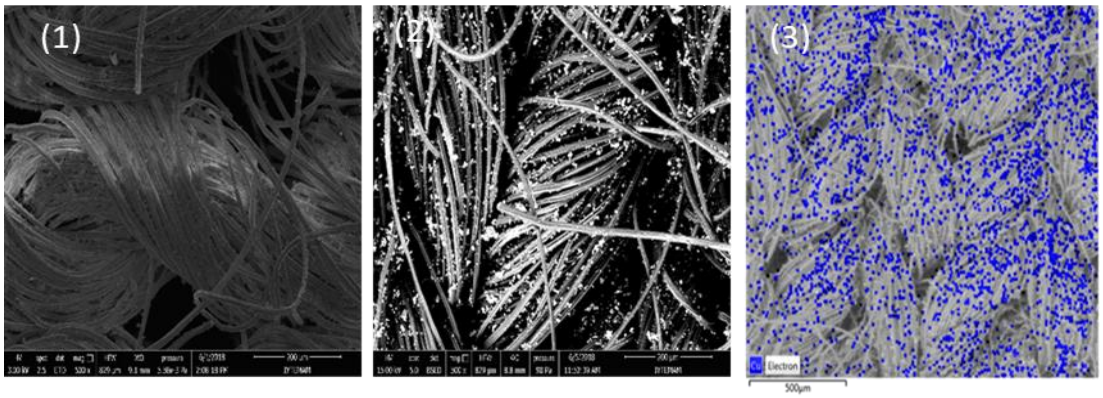

Figure 4. 41. SEM images of raw viscose fabric (1), Cu-BTC deposited viscose fabric(2), elemental mapping of Cu-BTC deposited viscose fabric(3).

According to the SEM images, the Cu particles are obviously shown in the related figure, and hence, the deposition process was successfully achieved.

FT-IR results of Cu-BTC, raw viscose fabric and Cu-BTC deposited viscose fabric are given in Figure 4. 42.

The peaks around 728, 1371 and 1644 cm^{-1} refer to the characteristic peaks of Cu-BTC and the results of FT-IR spectra show that deposition of Cu-BTC on viscose has been achieved successfully. Abdelhameed et al. carried out a study about the deposition of Cu-BTC on viscose and the characteristic peaks of viscose and Cu-BTC deposited viscose were observed around 730, 1000, 1370, and 1645 cm^{-1} (Abdelhameed et al., 2017). Similar results were observed in this study so that this study is in accordance with the literature.

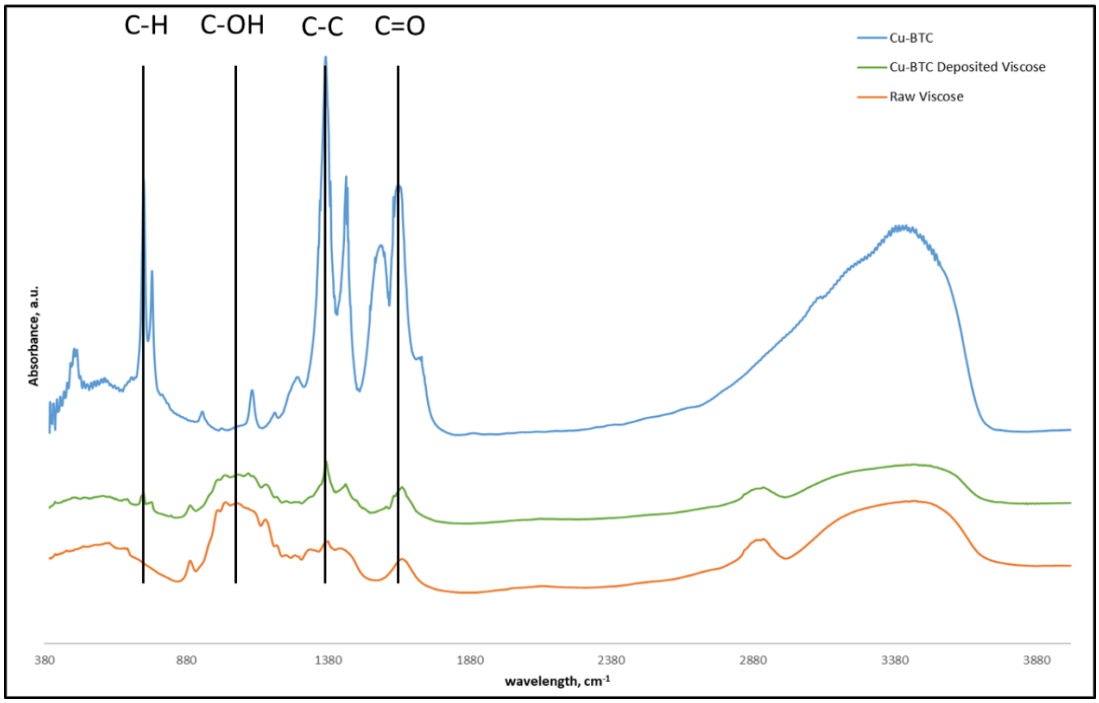

Figure 4. 42. FT-IR spectra of Cu-BTC, raw viscose fabric, Cu-BTC deposited viscose fabric.

ATR-IR analysis was also carried out for Cu-BTC, raw viscose fabric, Cu-BTC deposited viscose fabric and results are given in Figure 4. 43.

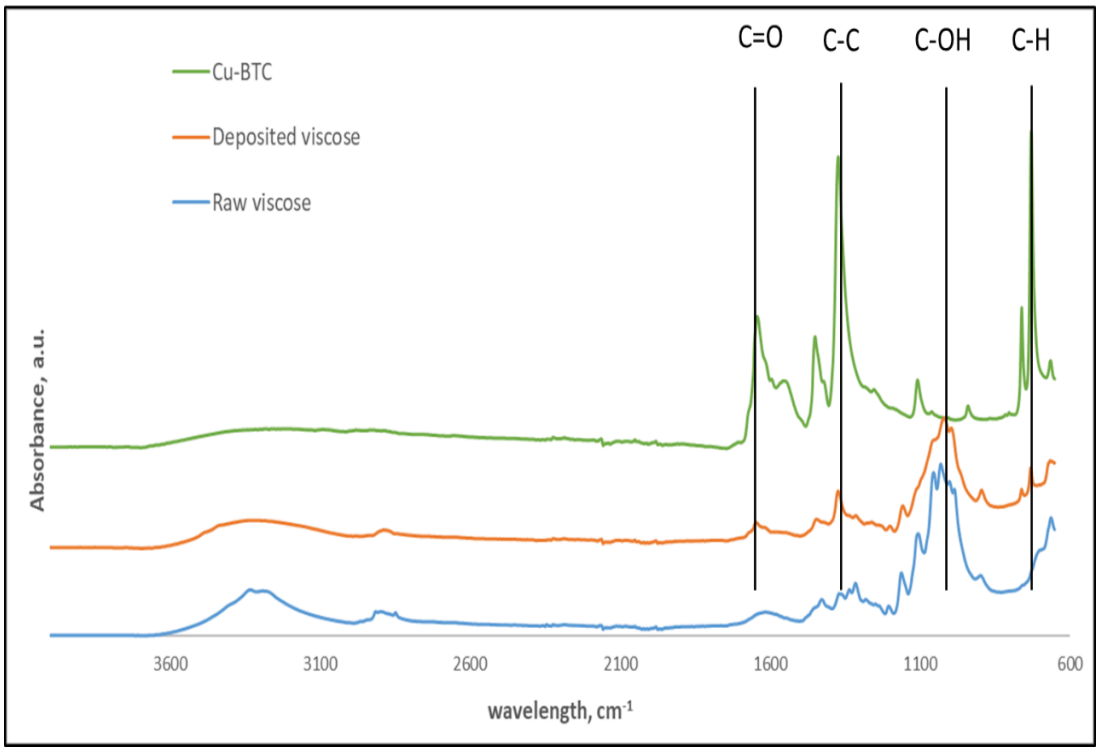

Figure 4. 43. ATR-IR spectra of Cu-BTC, raw viscose fabric, Cu-BTC deposited viscose fabric.

The characteristic peaks of raw viscose and Cu-BTC deposited viscose were observed at the similar wavelengths where the characteristic peaks of raw and Cu-BTC deposited pulp and cotton was observed. Therefore, the deposition of Cu-BTC was successfully achieved on the viscose.

XRD results of Cu-BTC, raw viscose fabric and Cu-BTC deposited viscose fabric are given in Figure 4. 44. The XRD results indicate that the raw viscose has amorphous structure. After Cu-BTC deposition the characteristic peaks of Cu-BTC was observed and these peaks imply that Cu-BTC has a crystal structure and the amorphous structure of raw viscose was conserved. According to the XRD results of Abdelhameed et al. study over Cu-BTC deposition on viscose, Cu-BTC deposited on viscose shows MOF strong sharp reflections at 2θ = 6.7°, 9.4°, 11.6°, 13.4°, and 19.1°, and weak peaks at 2θ = 17.4°, 20.1°, 25.9°, 29.4°, 35.3° and 39.2° (Abdelhameed et al., 2017). The similar results were observed in this study. Consequently, the results are in line with the literature.

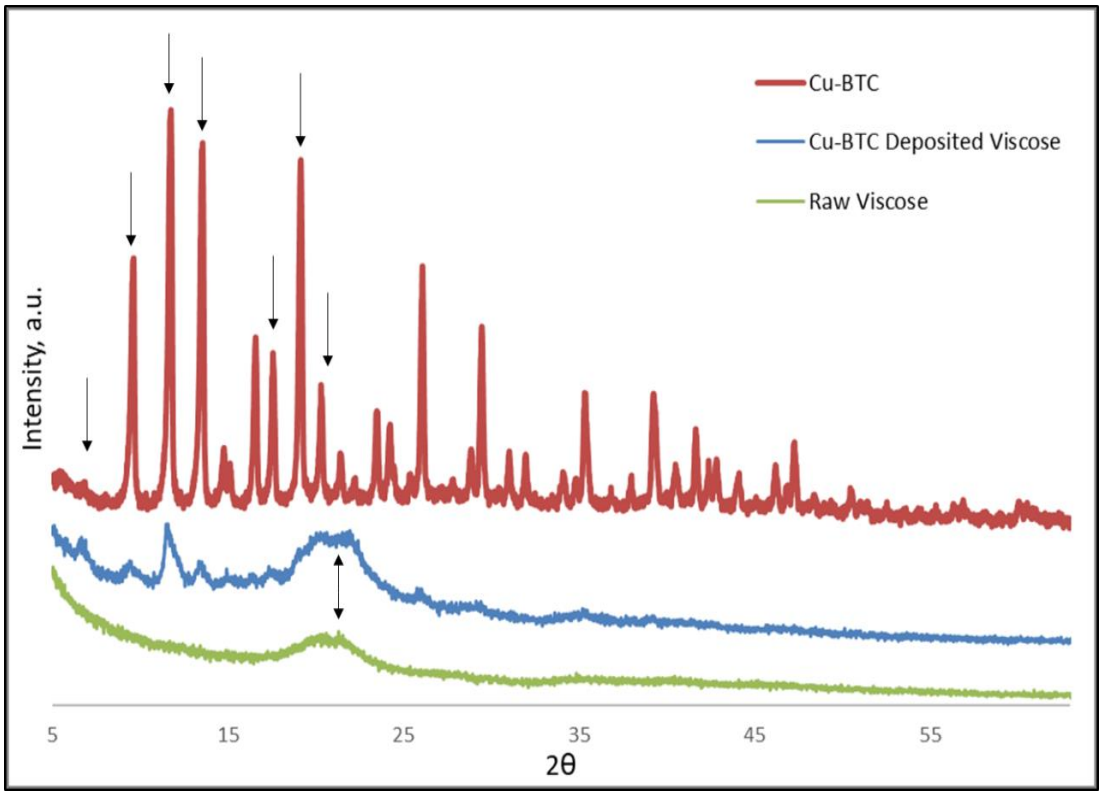

Figure 4. 44. XRD spectra of Cu-BTC, raw viscose fabric, Cu-BTC deposited viscose fabric.

NH_3 sensing properties of Cu-BTC deposited viscose was investigated and the results are shown in Figure 4. 45.

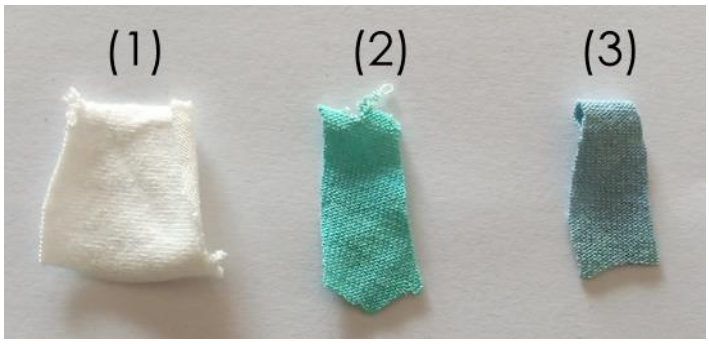

Figure 4. 45. Raw viscose (1), Cu-BTC deposited viscose (2), NH_3 exposed Cu-BTC deposited viscose (3).

According to the results, the color of Cu-BTC deposited viscose was changed from light blue to dark blue. Consequently, Cu-BTC deposited viscose has sensing property against NH_3.

4.4. Summary of the study

This study was summarized in Table 4. 1.

Table 4. 1. Summary of the study

Fiber Type	Pre-Treatmenr	Metal Source	Process	Temperature Effect	Cycle Number	Length of Fiber	NH3 Sensivity
Pulp	-	Copper Nitrate	Mixing with Cu-BTC Solution	Activation Temperature 85°C and 160°C	1) 6 h. 2) 12 h. 3) 24 h.	Long and Short	40 mL/min
Cotton	Carboxymethylation	Copper Nitrate	Mixing with Cu-BTC Solution	-	-	-	40 mL/min
	Carboxymethylation	Copper Acetate	Layer by Layer (with Water)	-	1) 4 cycle 2) 8 cycle 3) 12 cycle	-	40 mL/min
	Carboxymethylation	Copper Nitrate	Layer by Layer (with EtOH)	-	1) 5 cycle 2) 10 cycle 3) 15 cycle	-	40 mL/min
Viscose	-	Copper Nitrate	Mixing with Cu-BTC Solution	-	-	-	40 mL/min

CHAPTER 5

CONCLUSION

Cu-BTC was synthesized and deposited on the different substrates which are pulp, cotton, and viscose fibers. In this context, the effects of length of pulp fibers, stirring and temperature were investigated. There was not a significant effect of these parameters on the deposition efficiency of Cu-BTC on pulp fibers. The effects of carboxymethylation and deposition methods over the Cu-BTC deposition on the cotton were investigated. Two different carboxymethylation methods were used and there was not a major difference between the carboxymethylated cotton by these methods so that the carboxymethylation methods did not have importance. Three different Cu-BTC deposition method were tested for cotton and among them, layer by layer method show higher efficiency.

A characterization study was performed to comprehend whether the deposition of Cu-BTC was achieved successfully or not. In this context, the surface morphology, framework vibration, and crystalline structures of Cu-BTC and all Cu-BTC deposited substrates were analyzed via SEM, FT-IR, ATR-IR, and XRD analyses, respectively. Consequently, the results of the characterization study revealed that the Cu-BTC was deposited on the pulp, cotton fibers, and viscous successfully. The effect of deposition time for short and long pulp was investigated and it was found that 12 hours was enough for the deposition of Cu-BTC on the surface of pulp. Additionally, the effect of cycle number over the deposition of Cu-BTC by second and third method on the surface of cotton fabric. The optimum cycle numbers were found as 10 and 12 for the second and third method, respectively. Besides, their sensing properties against the NH_3 gas was investigated. The Cu-BTC deposited substrates showed sensing activity against NH_3 gas.

REFERENCES

Abdelhameed, R. M.; Emam, H. E. ; Rocha, J. ; Silva, A. M. S. ; Cu-BTC Metal-Organic Framework Natural Fabric Composites for Fuel Purification. *Fuel Processing Technology*, 159, 2017, 306–312.

Abuzalatı, O. ; Wong, D. ; Elsayed, M. ; Park, S. ; Kim, S. ; Sonochemical Fabrication of Cu(II) and Zn(II) Metal-Organic Framework Films on Metal Substrates. *Ultrasonics Sonochemistry,* 45, 2018, 180-188.

Astruc, D. ; Lu, F. ; Aranzaes, J. R. ; Nanoparticles as Recyclable Catalysts: The Frontier between Homogeneous and Heterogeneous Catalysis. *Angewandte Chemie International Edition*, *44*, 2005, 7852-7872.

Batten, S. R. ; Champness, N. R. ; Chen, X-M; Garcia-Martinez, J; Kitagawa, S; Öhrström, L; O'Keeffe, M; Suh, MP; Reedijk, J. "Terminology of metal–organic frameworks and coordination polymers (IUPAC Recommendations 2013). *Pure and Applied Chemistry*, 85, 2013, 1715-1724.

Čejka, J. (2012). Metal-Organic Frameworks. Applications from Catalysis to Gas Storage. Edited by David Farrusseng. *Angewandte Chemie International Edition*, 51(20), 4782-4783.

Cunha, D. ; Ben Yahia, M. ; Hall, S. ; Miller, S. R. ; Chevreau, H. ; Elkaïm, E. ; Maurin, G. ; Horcajada, P. ; Serre, C. ; Rationale of Drug Encapsulation and Release from Biocompatible Porous Metal–Organic Frameworks. *Chemistry of Materials*, *25*, 2013, 2767-2776.

Davydovskaya, P. ; Pohle, R. ; Tawil, A. ; Feischer, M. ; Work Function Based Gas Sensing with Cu-BTC Metal-Organic Framework for Selective Aldehyde Detection, *Sensors and Actuators B: Chemical*, 187, 2013, 142-146.

Falcaro, P.; Ricco, R. ; Yazdi, A. ; Imaz, I., Furukawa, S. ; Maspoch, D. ; Ameloot, R. ; Evans, J. D. ; Doonan, C. J. ; Application of Metal and Metal Oxide Nanoparticles@ MOFs. *Coordination Chemistry Reviews*, *307*, 2016, 237-254.

Horcajada, P. ; Chalati, T. ; Serre, C. ; Gillet, B. ; Sebrie, C. ; Baati, T. ; Eubank, J. F. ; Heurtaux, D. ; Clayette, P. ; Kreuz, C. ; Chang, J. ; Hwang Y. K. ; Marsaud, V. ; Bories, P. ; Cynober, L. ; Gil, S. ; Férey, G. ; Couvreur, P. ; Gref, R. ; Porous Metal–Organic-Framework Nanoscale Carriers as a Potential Platform for Drug Delivery and Imaging. *Nature materials*, 9, 2010, 172.

Hosseini, M. S. ; Zeinali, S. ; Sheikhi, M. H. ; Fabrication of Capacitive Sensor Based on Cu-BTC (MOF-199) Nanoporous Film for Detection of Ethanol and Methanol Vapors. *Sensors and Actuators B,* 230, 2016, 9-16.

Justino, C. I. L. ; Freitas, A. C. ; Pereira, R. ; Duarte, A. C. ; Rosha Santos, T. A. P. ; Recent Decelopmnts in Recogitinon Elements for Chemical Sensors and Biosensors. *Trends in Analytical Chemistry*, 68, 2015, 2-17.

Kreno, L. E. ; Leong, K. ; Farha, O. K. ; Allendorf, M. ; Van Duyne, R. P. ; Hupp, J. T. ; Metal-Organic Framework Materials as Chemical Sensors. *Chemical Reviews*, 112, 2011, 1105-1125.

Lucena, F. R. S. ; Araujo, L. C. C. ; Rodrigues M. D. ; Silva, T. G. ; Pereira, V. R. A. ; Militao, G. C. G. ; Fontes, D. A. F. ; Rolim-Neto, P. J. ; Silva, F. F. ; Nascimento, S. C. ; Induction of cancer Cell Death by Apoptosis and Slow Release of 5-Fluoacil from Metal-Organic Frameworks Cu-BTC. *Biomedicine & Pharmacotherapy*, 67, 2013, 707–713.

Luebbers, M. T. ; Wu, T., Shen, L. ; & Masel, R. I. ; Trends in the Adsorption of Volatile Organic Compounds in a Large-Pore Metal− Organic Framework, IRMOF-1. *Langmuir*, 26, 2010, 11319-11329.

Neufeld, M. J. ; Harding, J. L. ; Reynolds M. M. ; Immobilization of Metal-Organic Framework Copper(II) Benzene 1,3,5-tricarboxylate (CuBTC) onto Cotton Fabric as a Nitric Oxide Release Catalyst. *Applied Materials & Interfaces*, 7, 2015, 26742-26750.

Nijem, N. ; Fu, K. ; Kelly, S. T. ; Swain, C. ; Leone, S. R. ; Gilles, M. K. ; HKUST-1 Thin Film Layer-by-Layer Liquid Phase Epitaxial Growth: Film Properties and Stability Dependence on Layer Number. *Crystal Gowth & Design*, 15, 2015, 2948-957.

Nobar, S. N. ; Cu-BTC Synthesis, Characterization and Preparation for Adsorption. *Materials Chemistry and Physics*, 213, 2018, 343-351.

Peterson, G. W. ; Britt, D. K. ; Sun, D. T. ; Mahle, J. J. ; Browe, M. ; Demasky, T, ; Smith, S. ; Jenkins, A. ; Rossin, A. ; Multifunctional Purification and Sensing of Toxic Hydride Gases by CuBTC Metal-Organic Framework. *Industrial & Engineering Chemistry Research*, 54, 2015, 3626-3633.

Pinto, S. ; Augusto, C. ; Hinestroza, J. P. ; In Situ Synthesis of a Cu-BTC Metal–Organic Framework (MOF 199) onto Cellulosic Fibrous Substrates : Cotton. *Cellulose*, 19, 2012, 1771–1779.

Pirzadeh, K. ; Ghoreyhi, A. A. ; Rahimnejad, M. ; Mohammadi, M. ; Electrochemical Synthesis, Characterization and Application of a Microstructure $Cu_3(BTC)_2$ Metal Organic Framework for CO_2 and CH_4 Separation. *Korean Journal of Chemical Engineering*, 35, 2018, 974-983.

Rowsell, J. L. ; Yaghi, O. M. ; Strategies for Hydrogen Storage in Metal–Organic Frameworks. *Angewandte Chemie International Edition*, *44*, 2005, 4670-4679.

Rubin, H. N. ; Neufeld, B. H. ; Reynolds, M. M. ; Surface-Anchored Metal-Organic Framework-Cotton Materia for Tunable Antibacterial Copper Delivery. *Applied Materials & Interfaces*, 10, 2018, 15189-15199.

Siegle, S. ; Kaskel, S. ; Crystal Growth of the Metal-Organic Framework Cu3(BTC)2 on the Surface of Pulp Fibers. *Advanced Engineering Materials,* 3, 2009, 93–95.

Tranchemontagne, D. J. ; Mendoza-Cortés, J. L. ; O'Keeffe, M. ; & Yaghi, O. M. ; Secondary Building Units, Nets and Bonding in the Chemistry of Metal–Organic frameworks. *Chemical Society Reviews*, 38, 2009, 1257-1283.

Woellner, M. ; Hausdorf, S. ; Klein, N. ; Mueller, P. ; Smith, M. W. ; Kaskel, S. ; Adsorption and Detecdion of Hazardous Trace Gases by Metal-Organic Frameworks. *Advanced Materials*, 30, 2018, 1346-1370.

Xiao, F. ; Song, J. ; Gao, H., Zan, X. ; Xu, R. ; Duan, H. ; Coating Graphene Paper with 2D-Assembly of Electrocatalytic Nanoparticles: a Modular Approach Toward High-Performance Flexible Electrodes. *Acs Nano*, 6, 2005, 100-110.

Xiao, J. ; Fang, L. ; Benard, P. ; Chahine, R. ; Parametric Study of Pressure Swing Adsorption Cycle for Hydrogen Purification Using Cu-BTC. *International Journal of Hydrogen Energy*, 43, 2018, 13962-13974.

Yamauchi, M. ; Kobayashi, H. ; Kitagawa, H. ; Hydrogen Storage Mediated by Pd and Pt Nanoparticles. *ChemPhysChem*, 10, 2009, 2566-2576.

Yang, Y. ; Dong, H. ; Wang, Y. ; He, C. ; Wang, Y. ; Zhang, X. ; Synthesis of Octahedral like Cu-BTC Derivatives Derived from MOF Calcined under Different Atmosphere for Application in CO Oxidation. *Journal of Solid State Chemistry*, 258, 2018, 582–587.

Zhuang, J.; Kind, M. ; Grytz, C. M. ; Farr, F. ; Diefenbach, M. ; Tussupbayev, S. ; Holthausen, M. C. ; Terfort, A. ; Insight into the Oriented Growth of Surface-Attached Metal−Organic Frameworks: Surface Functionality, Deposition Temperature, and First Layer Order. *Journal of the American Chemical Society*, 137, 2015, 8237-8243.